nature medicine

Article

https://doi.org/10.1038/s41591-024-03109-0

Adoptive transfer of personalized neoantigen-reactive TCR-transduced T cells in metastatic colorectal cancer: phase 2 trial interim results

Received: 22 January 2024

Accepted: 4 June 2024

Published online: 11 July 2024

Check for updates

Maria Parkhurst ✉, Stephanie L. Goff, Frank J. Lowery, Rachel K. Beyer, Hyunmi Halas, Paul F. Robbins, Todd D. Prickett, Jared J. Gartner, Sivasish Sindiri, Sri Krishna, Nikolaos Zacharakis, Lien Ngo, Satyajit Ray, Alakesh Bera, Ryan Shepherd, Noam Levin, Sanghyun P. Kim, Amy Copeland, Shirley Nah, Shoshana Levi, Neilesh Parikh, Mei Li M. Kwong, Nicholas D. Klemen, James C. Yang & Steven A. Rosenberg

Adoptive cell transfer (ACT) with neoantigen-reactive T lymphocytes can mediate cancer regression. Here we isolated unique, personalized, neoantigen-reactive T cell receptors (TCRs) from tumor-infiltrating lymphocytes of patients with metastatic gastrointestinal cancers and incorporated the TCR α and β chains into gamma retroviral vectors. We transduced autologous peripheral blood lymphocytes and adoptively transferred these cells into patients after lymphodepleting chemotherapy. In a phase 2 single-arm study, we treated seven patients with metastatic, mismatch repair-proficient colorectal cancers who had progressive disease following multiple previous therapies. The primary end point of the study was the objective response rate as measured using RECIST 1.1, and the secondary end points were safety and tolerability. There was no prespecified interim analysis defined in this study. Three patients had objective clinical responses by RECIST criteria including regressions of metastases to the liver, lungs and lymph nodes lasting 4 to 7 months. All patients received T cell populations containing ≥50% TCR-transduced cells, and all T cell populations were polyfunctional in that they secreted IFNγ, GM-CSF, IL-2 and granzyme B specifically in response to mutant peptides compared with wild-type counterparts. TCR-transduced cells were detected in the peripheral blood of five patients, including the three responders, at levels ≥10% of $CD3^+$ cells 1 month post-ACT. In one patient who responded to therapy, ~20% of $CD3^+$ peripheral blood lymphocytes expressed transduced TCRs more than 2 years after treatment. This study provides early results suggesting that ACT with T cells genetically modified to express personalized neoantigen-reactive TCRs can be tolerated and can mediate tumor regression in patients with metastatic colorectal cancers. ClinicalTrials.gov registration: NCT03412877.

Surgery Branch, NCI, NIH, Bethesda, MD, USA. ✉e-mail: maria_parkhurst@nih.gov

https://doi.org/10.1038/s41591-024-03109-0

Table 1 | Patient treatment summary

Resection number	Age and sex	Diagnosis	MMR status	Sites of disease	Number of therapies before resection	Source of TCR	Number of cells infused	Number of IL-2 doses	Number of pembrolizumab doses	OR
4293	53, female	Colon	Proficient	Colon, lungs, vertebra	2	Lung	1.5×10^{11}	4	None	NR
4367	40, male	Colon	Proficient	Liver, lungs, soft tissue	4	SQ	1.5×10^{11}	4	2	NR
4378	37, male	Rectal	Proficient	Liver, lungs	2	Lung	1.5×10^{11}	5	4	PR (6 months)
4405	54, female	Rectal	Proficient	Lungs, liver	4	Liver	1.1×10^{11}	3	4	PR (7 months)
4420	53, male	Colon	Proficient	Liver, lungs, lymph nodes	2	Lymph node	1.2×10^{11}	2	1	PR (4 months)
4469	39, male	Colon	Proficient	Liver, lungs, lymph nodes	1/3[a]	Lung	6.0×10^{10}	2	None	NR
4484	43, female	Colon	Proficient	Lung, liver, peritoneum, left fallopian tube, lymph nodes	8	Lung	1.1×10^{11}	4	2	NR

[a]Three courses of the same chemotherapy regimen. OR, objective response; PR, partial response; NR, no response; SQ, sub-cutaneous nodule.

During cancer development, tumors accumulate genetic abnormalities including point mutations, reading frameshift mutations, stop codon mutations, DNA insertions and deletions, and/or chromosomal translocations, all of which can result in the production of variant proteins. Some of these can be processed into small peptides or neoepitopes, presented on cell surfaces in the context of major histocompatibility complex (MHC) molecules and recognized by T lymphocytes. These neoantigens represent ideal tumor-associated T cell targets as they are not expressed in normal tissues. We previously showed that approximately 80% of patients with gastrointestinal cancers harbor neoantigen-reactive T lymphocytes within their tumors[1]. We also observed that only 1–2% of mutations are antigenic, and with rare exceptions, all the specific human leukocyte antigen (HLA)-restricted neoantigenic determinants are unique to the autologous patient.

Adoptive cell transfer (ACT) with tumor-infiltrating lymphocytes (TILs) selected for the presence of neoantigen-reactive T cells has previously been shown to mediate tumor regression in individual patients with metastatic melanoma, cholangiocarcinoma (bile duct tumors), cervical cancer and breast cancer[2–5]. However, fresh TILs are often highly differentiated, and the protocol for expanding TILs to therapeutic levels drives cells to become further exhausted. Multiple studies in mice and humans suggest that transfer of tumor-antigen-specific T lymphocytes with less differentiated phenotypes is more effective at inducing tumor regression and is associated with superior persistence than those that are more exhausted[6–8]. In addition, nonspecific stimulation of CD3 as a part of cell manufacturing protocols can lead to overgrowth of bystander cells such that final patient products may not contain high percentages of neoantigen-reactive T cells.

Previous trials in which patients were treated with ACT using retrovirally modified peripheral blood lymphocytes (PBLs) expressing T cell receptors (TCRs) targeting non-mutated tumor-associated proteins including melanocyte differentiation antigens (MART-1 and gp100)[9] and a cancer-testis antigen (NY-ESO-1)[10,11] showed that TCR-transduced lymphocytes can mediate tumor regression in patients with melanoma and synovial cell sarcoma and that the transduced cells can persist in vivo for long periods of time after treatment. However, major on-target, off-tumor toxicities have been observed in patients treated with TCR-transduced PBLs targeting non-mutated antigens including MART-1 and gp100 (ref. 9), CEA (ref. 12) and MAGE-A3 (refs. 13,14), highlighting the need to develop neoantigen-directed therapies specific for tumor cells.

To overcome the challenges posed by T cell differentiation and overgrowth of bystander cells, we initiated a phase 2 single-arm clinical trial in which patients with any type of metastatic cancer are treated with autologous PBLs genetically modified to express neoantigen-reactive TCRs (ClinicalTrials.gov identifier: NCT03412877). Here we report the manufacture and characterization of ACT as well as early findings from this trial, focusing on patients with mismatch repair (MMR)-proficient colorectal cancers. We did not have a prespecified interim analysis, but we believe it is important to report these early findings as the patient responses described here represent proof of principle that an approach using a personalized TCR strategy targeting random somatic mutations may lead to tumor regression, an observation that, to our knowledge, has not previously been reported.

Results

Clinical trial overview

Patients described herein were enrolled in the clinical trial between September 2018 and March 2023, and the study is ongoing. Patients with metastatic epithelial cancers were treated with autologous PBLs genetically modified to express personalized neoantigen-reactive TCRs derived from TILs. We produced good manufacturing practice (GMP)-quality retroviral products encoding the TCR α and β chains, transduced the patient's PBLs and reinfused them into the patient after preconditioning with a non-myeloablative lymphodepleting chemotherapy regimen consisting of cyclophosphamide and fludarabine. Patients also received four doses of pembrolizumab every 3 weeks starting before cell transfer and cytokine support after infusion with high-dose interleukin-2 (IL-2) as tolerated. We treated seven patients with metastatic MMR-proficient colorectal cancers with personalized neoantigen-reactive TCR-transduced PBLs as first-line ACT (Table 1), all of whom had previously been treated with at least two courses of chemotherapy (Supplementary Table 1).

Identification of neoantigen-reactive TCRs

We used two approaches to identify neoantigen-reactive TCRs. In the first approach, each patient underwent a resection of metastatic lesion(s). Tumors were dissected into small fragments from which T cells were allowed to emigrate and expand in the presence of high-dose IL-2 as previously described[15]. At the same time, we isolated DNA and RNA from the tumor and normal PBLs and performed whole exome sequencing (WES) and transcriptome sequencing (RNA-seq) to identify somatic mutations. We then screened each somatic variant for

recognition by T cells from each TIL fragment by coculturing the TILs with autologous dendritic cells (DCs) loaded with tandem minigene (TMG) RNAs or synthetic peptides encoding all the mutations as previously described[1,4]. We then performed fluorescence-associated cell sorting (FACS) of individual T cells from reactive fragments based on upregulation of activation markers (4-1BB and/or OX40) and carried out targeted sequencing of cDNA to identify TCR α and β chains. We then constructed and evaluated retroviral vectors encoding the potential TCRs. In these vectors, the human TCR Vα and Vβ chains were grafted onto murine constant regions to prevent mispairing with endogenous TCRs as previously described[16]. This is the approach we used to identify TCRs for six of the seven patients (4293, 4367, 4378, 4405, 4469 and 4484), and an outline of this strategy is presented in Fig. 1a.

As one example of this neoantigen TCR discovery platform, for patient 4378, we screened 24 TIL fragment cultures against 125 mutations and identified multiple populations that appeared to contain $CD8^+$ T lymphocytes that recognized TMG constructs 1 and 2 in our original screening assays (Fig. 1b). We deconvoluted the TMGs by evaluating recognition of individual 25-amino-acid peptides encoded by the TMGs (Supplementary Fig. 1: representative results for F18 and F12) and identified the neoantigens, mutant GCLM (TMG1), an enzyme involved in glutathione synthesis, and mutant ALDH2 (TMG2), an aldehyde dehydrogenase involved in alcohol metabolism (Supplementary Fig. 1). To identify mutant-GCLM-reactive TCRs, we cocultured TIL fragments with TMG1-electroporated DCs (Fig. 1c and Supplementary Fig. 2a), sorted single $CD8^+4\text{-}1BB^+$ T lymphocytes and identified one dominant TCR: TRAV2/TRBV7-9. Similarly, to identify mutant ALDH2-reactive TCRs, we cocultured TIL fragments with TMG2-electroporated DCs (Fig. 1d and Supplementary Fig. 2b), sorted single $CD8^+4\text{-}1BB^+$ T lymphocytes and identified one dominant TCR: TRAV41/TRBV20-1. For each of these TCRs, we constructed retroviral vectors, transduced PBLs from healthy donors and measured IFNγ secretion in response to the relevant TMGs and mutant and wild-type 25-amino-acid peptides (Fig. 1c,d). The TRAV2/TRBV7-9 TCR mediated recognition of mutant GCLM, and the TRAV41/TRBV20-1 TCR mediated recognition of mutant ALDH2 (Fig. 1c,d). In addition, using the NetMHCpan MHC binding prediction algorithm, we made a series of short peptides from mutant GCLM and ALDH2 predicted to bind with high affinity to each of the patient's class I HLA molecules, evaluated recognition and identified minimal epitopes (Supplementary Fig. 3a). Finally, we identified the specific HLA restriction elements for each of these epitopes by pulsing short peptides onto COS-7 cells transiently transfected with each of the patient's class I HLA molecules (Supplementary Fig. 3b).

In our second approach for identifying neoantigen-reactive TCRs, used for patient 4420, single-cell digests were prepared from resected tumors, and individual T cells expressing CD8, PD-1, CD39 and TIGIT were sorted and sequenced to identify potential TCR α and β chains as previously described[17]. Retroviral vectors incorporating these TCRs were constructed, and transduced PBLs were screened for neoantigen reactivity. Six potential TCRs were identified, and one of these mediated recognition of mutant EXOC4, a protein involved in targeting exocytic vesicles to specific docking sites on the plasma membrane.

Five of the seven patients received TCRs derived exclusively from HLA class II-restricted $CD4^+$ T cells (Extended Data Table 1), one of whom (patient 4405) had a partial response to therapy lasting 7 months. In contrast, the two patients who received TCRs derived exclusively from HLA class I-restricted $CD8^+$ T cells (4378 and 4420; Extended Data Table 1) responded to therapy.

To determine whether the TCRs we identified had the potential to recognize tumor cells in vivo, we evaluated expression of the specific mutated genes in cancer cells derived from the original tumor resections. This was done by estimating the percentage of tumor cells bearing the mutation in each specimen via WES (cancer cell fraction (CCF)) and by estimating the level of mutant gene expression via RNA-seq (Table 2). Of the ten neoantigens that were targeted in these seven patients, five appeared to be clonal (4293 TP53, 4367 PIK3CA, 4378 ALDH2, 4405 MAGED2 and 4420 EXOC4) and four of these were within the top two quartiles of expression by RNA-seq (all except 4367 PIK3CA). The other five targets appeared to be subclonal with variable CCF values in different specimens (4378 GCLM, 4469 CREG1 and 4469 PLEC) or low CCF values in all of the sequenced fragments (4293 SMC3 and 4484 STK10). Overall, in five of the seven patients, we appeared to target at least one clonal mutation (4293, 4367, 4378, 4405 and 4420), three of whom (4378, 4405 and 4420) responded to therapy. No clinical responses were observed in the two patients for whom the administered TCRs only targeted subclonal mutations (4469 and 4484).

We also evaluated HLA loss of heterozygosity (LOH) in tumor samples and identified one specimen with clear evidence of HLA class I LOH (4469; Table 2). Although this patient did not respond to therapy, he was treated with two HLA class II restricted CD4-derived TCRs, so it is unclear whether this HLA LOH had a negative therapeutic impact.

Manufacture and characterization of clinical-grade retroviral supernatants and T cell products

One major difference between this clinical trial and every other gene therapy trial using gamma retroviruses was the use of retroviral products generated from transiently transfected 293GP cells (Extended Data Fig. 1). In other trials, large volumes of supernatants were required to treat multiple patients with a single product, and the Food and Drug Administration mandated the generation of stable packaging cell lines. The production and validation of these lines and subsequent retroviral products are impractical for generating small-scale personalized products intended for the treatment of a single patient. Therefore, we developed Food and Drug Administration-approved processes for producing small batches of retroviral products in-house via transient transfection of 293GP cells with TCR and RD114 *env*-containing plasmids under GMP. Individual vector supernatants were generated for each TCR, and all required quality control testing for immediate clinical use was completed in-house. All vectors passed all quality control tests (Extended Data Table 2 and Supplementary Table 2).

To generate TCR-transduced cell products, cryopreserved peripheral blood mononuclear cells (PBMCs) were thawed, stimulated with IL-2 and anti-CD3, and transduced with GMP-quality retroviral products 2 days later. For some patients, $CD4^+$ or $CD8^+$ T cells were enriched before the transduction by depleting cells expressing the opposite coreceptor. Then, 10 days after the initial stimulation, transduced cells were restimulated with irradiated feeder cells, IL-2 and anti-CD3 to further expand the cells. Subsequently, 14 days after the second stimulation, the cells were collected, combined (if more than one TCR population was generated) and adoptively transferred into the autologous patient. All of the cell products given to patients passed all of the release testing criteria in accordance with the Certificate of Analysis (COA) including sterility, potency and viability tests. In addition, vector copy numbers on all final cell products were within the cell COA limit of an average ≤5 copies per cell (Extended Data Table 3).

Multiple studies in mice and humans suggest that tumor-antigen-specific T lymphocytes with less differentiated phenotypes are more effective at inducing tumor regression than exhausted cells[6–8,18]. To determine whether phenotypic characteristics correlated with clinical response, we characterized the phenotypes of the adoptively transferred neoantigen-reactive TCR cell products by evaluating expression of CD3, CD4, CD8, CD45RO, CD62L, CD27, CD39 and CD69 on the TCR-transduced cells. Examples of our FACS gating strategies are presented in Fig. 2a for the GCLM and ALDH2 TCRs from patient 4378. Overall, there was considerable variability in TCR transduction efficiency between patients and TCRs (Extended Data Table 3), ranging from ~22% to 84%, but no apparent correlation with patient response was observed. In all patients, the majority of infused cells had an effector memory phenotype ($CD45RO^+CD62L^-$) and did not express CD27, a marker associated with less differentiated cells (Extended Data Table 3).

https://doi.org/10.1038/s41591-024-03109-0

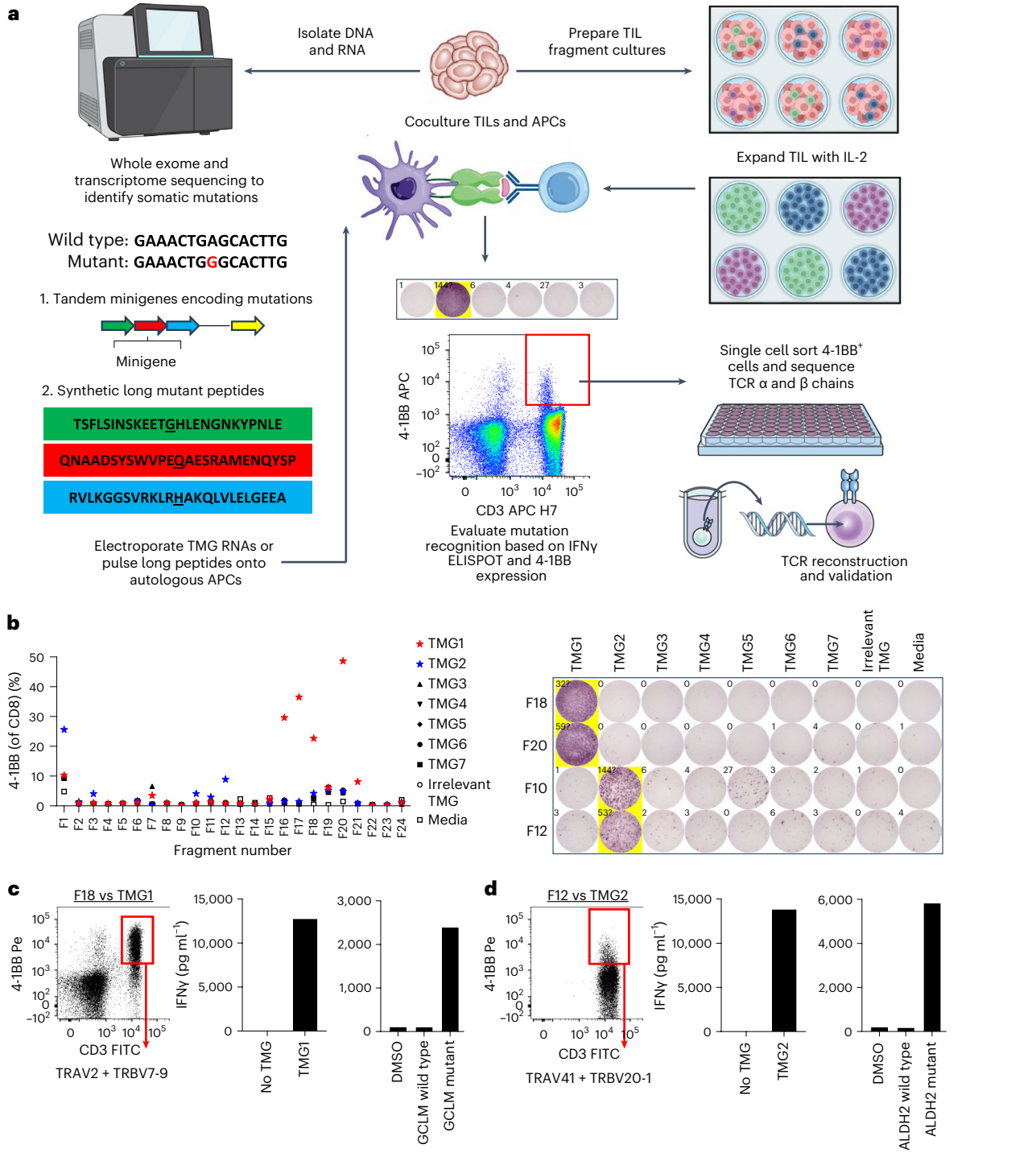

Fig. 1 | Identification of neoantigen-reactive TCRs. a, Schematic diagram of a neoantigen-reactive TCR discovery platform based on upregulation of activation markers by TIL fragment cultures in response to autologous DCs electroporated with RNAs or pulsed with synthetic peptides encoding tumor-associated mutations. **b**, Identification of neoantigen-reactive CD8$^+$ T cells from a patient with colon cancer (4378). A total of 24 TIL subcultures from patient 4378 were cocultured overnight with autologous DCs transfected with an irrelevant TMG or the indicated TMG encoding mutations identified by WES. TILs were also cultured without DCs (media) as negative controls or with phorbol 12-myristate 13-acetate and ionomycin as positive controls. T cell responses were measured by flow-cytometric analysis of 4-1BB on CD8$^+$ T cells (left) and IFNγ enzyme-linked immunosorbent spot (ELISPOT) (right, four example fragments). **c**,**d**, T cells from F18 were cocultured with autologous DCs electroporated with TMG1 RNA (**c**), and T cells from F12 were cocultured with autologous DCs electroporated with TMG2 RNA (**d**). After gating on CD8$^+$ cells, 96 individual CD3$^+$ 4-1BB$^+$ cells, as indicated by the red boxes in the top right of the FACS plots, were sorted into a 96-well plate, and single-cell RT-PCR was performed on the contents of each well to amplify TCRα and β chains. From each fragment, one dominant TCR was identified. PBLs from healthy donors were genetically modified via retroviral transduction to express the TCRs and were then cocultured overnight with relevant TMG-electroporated or peptide-pulsed DCs. T cell responses were measured by IFNγ ELISA, and recognition of WT and mutant GCLM (**c**) or ALDH2 (**d**) by T cells expressing each of the respective TCRs is shown. Images in **a** created in part with BioRender.com. APC, allophycocyanin; FITC, fluorescein isothiocyanate; Pe, phycoerythrin.

https://doi.org/10.1038/s41591-024-03109-0

Table 2 | Neoantigen and HLA expression in tumors resected before T cell therapy

Resection number	Neoantigen	Number of specimens analyzed for CCF	Mean CCF	CCF range	Number of specimens analyzed for expression	Expression quartile	Mean expression[a]	Expression range	Number of specimens analyzed for LOH[b]	HLA class I LOH
4293	TP53 (Y236S)	2	0.997	0.994–1	2	4	4.4	4.3 to 4.4	2	Inconclusive
	SMC3 (S900delinsSM)		0.184	0.172–0.196		4	3.2	3.2 to 3.2		
4367	PIK3CA (N345K)	3	0.975	0.972–0.978	4	2	−1	−9 to 1.7	3	No LOH
4378	GCLM (D177N)	7	0.281	0–0.987	6	2	0.9	0.3 to 1.7	7	4 no LOH, 3 inconclusive (2 specimens nearly clonal, 5 specimens 0)
	ALDH2 (P184L)		0.988	0.972–1.0		4	3.8	3.4 to 4.3		
4405	MAGED2 (K150E)	4	0.993	0.990–0.995	5	4	4.4	4.1 to 4.8	4	3 no LOH, 1 inconclusive
4420	EXOC4 (K91N)	3	0.99	0.985–0.993	4	3	2.3	2.0 to 2.7	3	2 no LOH, 1 inconclusive
4469	CREG1 (D67H)	4	0.713	0.447–0.912	5	3	2.4	2.1 to 2.7	4	LOH, loss of alleles HLA-A*02:11, HLA-B*51:01, HLA-C*14:02
	PLEC (E4174K)		0.915	0.741–0.980		4	3.9	3.7 to 4.2		
4484	STK10 (R867L)	4	0.293	0–0.430	4	4	2.5	2.4 to 2.6	4	3 no LOH, 1 inconclusive (3 specimens averaged 0.390, 1 specimen 0)

[a]Expression: normalized $\log_2$ transcripts of the gene per million. [b]LOH in the HLA class I locus.

In terms of CD39 and CD69, there was considerable patient-to-patient variability with the double-negative cell fraction ranging from 11% to 76% of the TCR-transduced cells. Of potential interest, we noted that both patients who received CD8-derived TCRs (4378 and 4420) had partial clinical responses to their TCR therapies, and the adoptively transferred TCR-transduced cells in these two patients contained the highest percentages of $CD39^{-}CD69^{-}$ cells.

We also evaluated the phenotypes of pre-treatment PBLs used for transductions (Supplementary Fig. 4), and although there was considerable patient-to-patient variability, no markers correlated with clinical response.

For each of the adoptively transferred cell products, we evaluated function by measuring IFNγ secretion in response to titrated amounts of mutant and wild-type peptides. Examples of these assays are presented in Fig. 2b for the combined GCLM and ALDH2 TCR product for patient 4378. All T cell products exhibited mutant peptide specificity (Fig. 2b and Supplementary Fig. 5). In addition to IFNγ, we measured IFNα, granulocyte-macrophage colony-stimulating factor (GM-CSF), IL-2, IL-4, IL-5, IL-6, IL-9, IL-10, IL-12, IL-17α, IL-21, tumor necrosis factor-α (TNFα), granzyme B, perforin and monocyte chemoattractant protein-1 (MCP-1) in coculture supernatants, and examples of these assays are presented in Fig. 2c for the 4378 product. Cell products for every patient specifically secreted GM-CSF, IL-2 and granzyme B in response to mutant peptides (Fig. 2c and Supplementary Fig. 6). For all the other cytokines, chemokines and perforin, we noted considerable variabilities between patients, but none appeared to correlate with clinical response.

Clinical responses

We treated seven patients with metastatic MMR-proficient colorectal cancers with personalized neoantigen-reactive TCR-transduced PBLs as first-line ACT (Table 1), and three patients (4378, 4405 and 4420) experienced short-duration partial responses as described by Response Evaluation Criteria in Solid Tumours (RECIST) 1.1 criteria including regression of metastases to the liver, lung and lymph nodes (Fig. 3 and Supplementary Fig. 7). Median progression-free survival was 4.6 months. All patients were taken off study at time of progression to pursue other standard or experimental therapies.

A clinical course description for each patient is provided in Supplementary Information.

Toxicities

One patient (4367) experienced a grade 4 severe cytokine release syndrome attributed to both cells and IL-2, which resolved with supportive care including steroids and tocilizumab; ambulatory discharge occurred on day 21. All patients developed grade 3/4 cytopenias, as expected with the lymphodepleting design of the therapy. One patient developed a transient acute bleeding diathesis that resolved with blood and blood product transfusions. There were no treatment-related deaths.

Exploratory analyses of post-transfer PBL

For each patient, we evaluated persistence and peak T cell expansion (Cmax) of the TCR-transduced cells in post-treatment PBMC. An example of our FACS analysis strategy is shown in Extended Data Fig. 2 for the GCLM and ALDH2 TCRs for patient 4378. In five of the seven patients, we could detect TCR-transduced cells at every time point for which PBMC samples were available (Fig. 4). For patients 4293 and 4367, neither of whom responded to therapy, we did not reliably detect TCR-transduced cells in day 41 post-ACT PBL. For peak T cell expansion, we estimated the following maximum percentages of all TCR-transduced cells on the indicated day post-ACT: 4293 (42%, day 6), 4367 (55%, day 5), 4378 (58%, day 10), 4405 (79%, day 6), 4420 (84%, day 15), 4469 (62%, day 5) and 4484 (58%, day 11). Comparing these Cmax values between responders (4378, 4405 and 4420) and non-responders (4293, 4367, 4369 and 4484), an unpaired *T*-test yielded $P = 0.07$. As such, no clear correlation was observed between length of persistence or peak T cell expansion and response to therapy.

https://doi.org/10.1038/s41591-024-03109-0

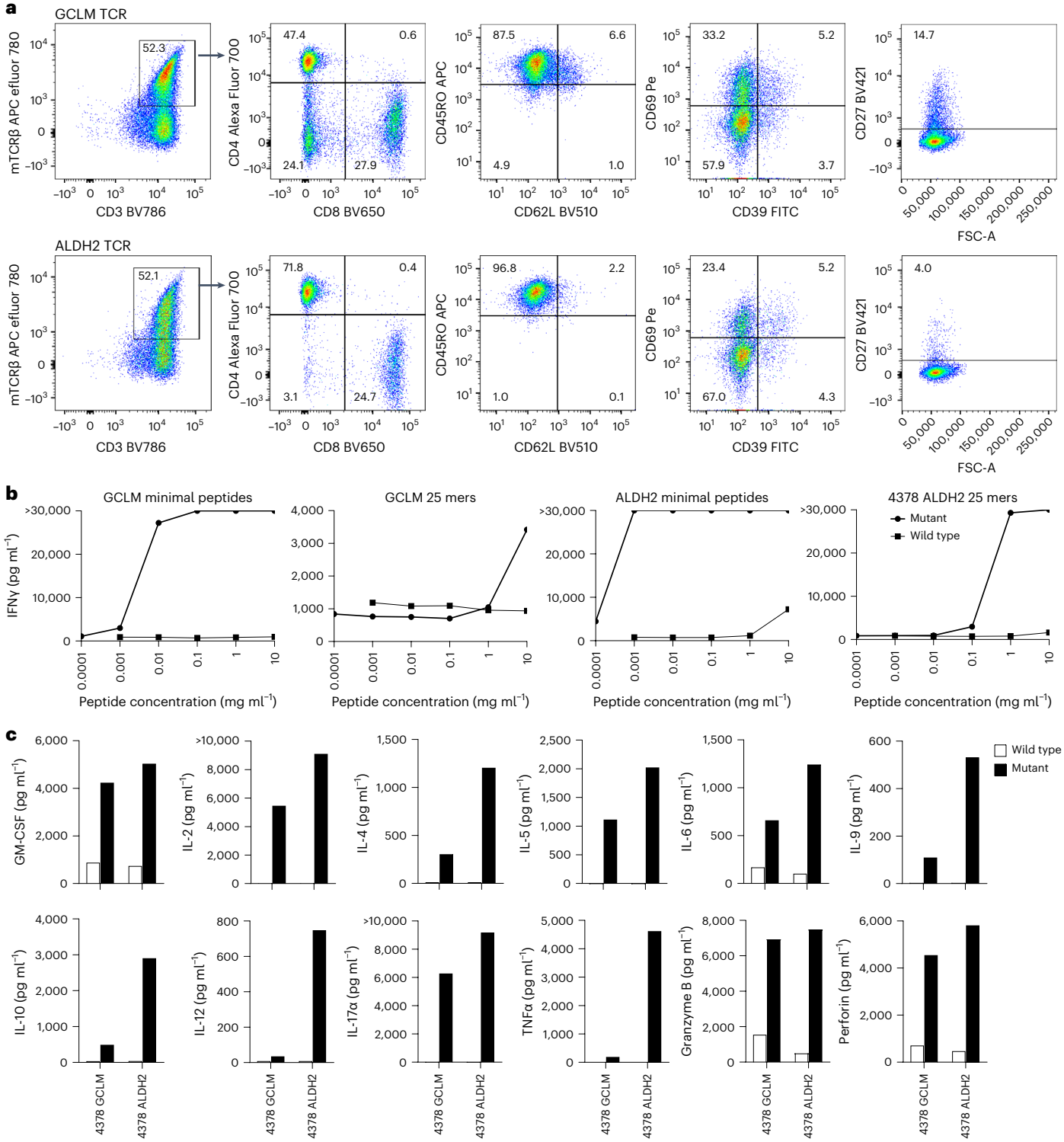

Fig. 2 | Characterization of TCR-transduced cells for patient treatment. **a**, Examples of FACS gating strategies to define phenotypes of adoptively transferred T cell products for GCLM and ALDH2 TCRs from patient 4378. Cryopreserved samples frozen on the day of adoptive transfer were thawed and rested overnight in the presence of 600 IU ml^{-1} IL-2 before FACS. For patients treated with two TCRs, individual cell products were evaluated before combination for infusion. Cells were stained with antibodies against human CD3, CD4, CD8, CD45RO, CD62L, CD27, CD39 and CD69, and against the murine TCRβ chain that identified the transduced cells. Phenotypic evaluation was performed on lymphocyte-size gated, live (propidium iodide (PI) negative), CD3$^+$, murine TCRβ$^+$ cells. **b**, Examples of functional analyses of adoptively transferred T cell products for GCLM and ALDH2 TCRs from patient 4378. Cryopreserved samples frozen on the day of adoptive transfer were thawed and rested overnight in the presence of 600 IU ml^{-1} IL-2 before FACS. For patients treated with two TCRs, the combined cell product given to the patient was evaluated. Levels of IFNγ in supernatants from cocultures of T cells with peptide-pulsed autologous DCs were measured by ELISA. For patients who received TCRs derived from HLA class I-restricted CD8 cells, such as the GCLM and ALDH2 TCRs presented here, IFNγ was measured in response to titrated concentrations of both 25-amino-acid wild-type and mutant peptides as well as against minimal epitopes. **c**, Examples of multi-cytokine functional analyses of adoptively transferred T cell products for GCLM and ALDH2 TCRs from patient 4378. Supernatants from cocultures of infused T cell products and autologous DCs pulsed with 1 μg ml^{-1} of wild-type and mutant minimal peptides were evaluated for levels of the indicated cytokines and chemokines using MACSPlex kits from Miltenyi Biotech.

https://doi.org/10.1038/s41591-024-03109-0

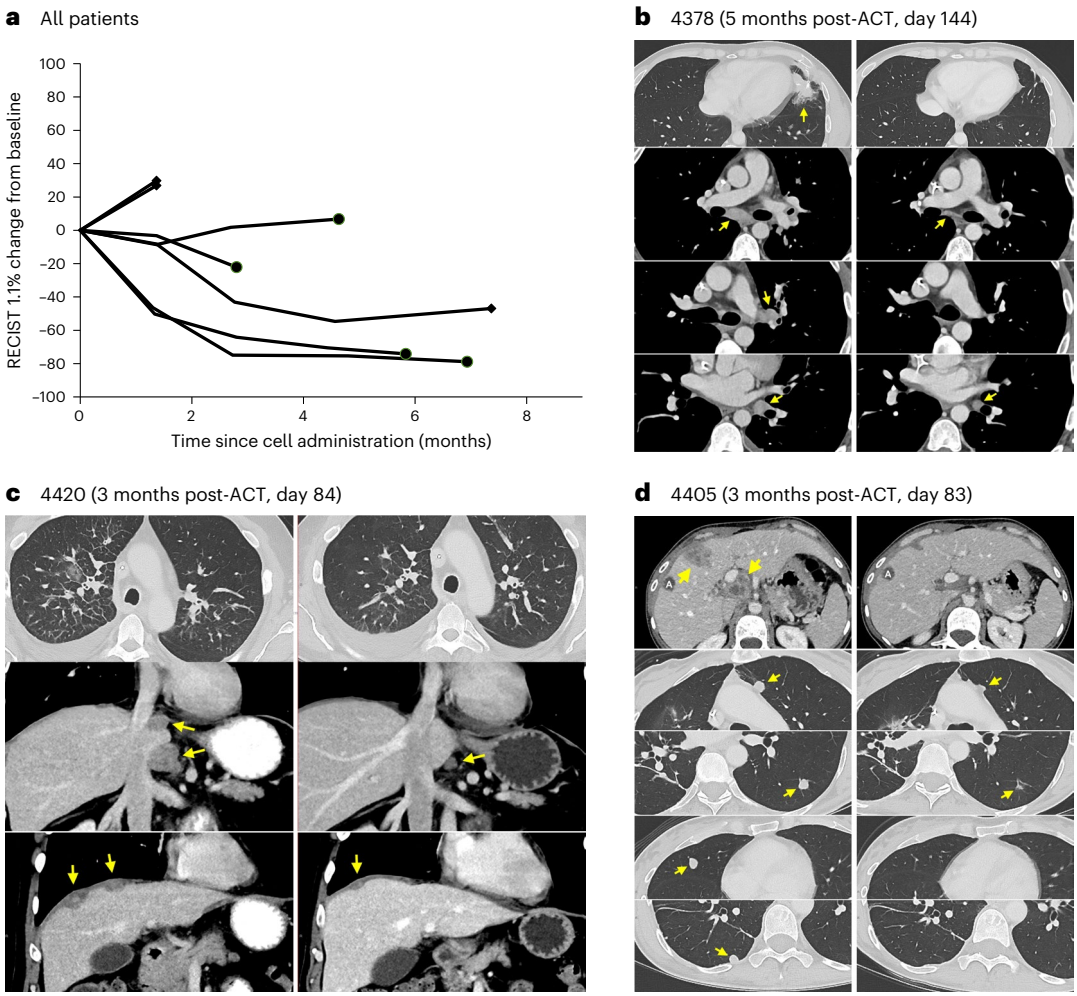

Fig. 3 | Clinical responses to therapy with autologous PBLs retrovirally transduced with neoantigen-reactive TCRs. a, Spider plot showing percentage change in RECIST 1.1 target tumor measurements from time of cell infusion. The shape of the final point indicates the mode of progressive disease (circles, new site of disease; diamonds, increase in non-target disease). **b**–**d**, Cross-sectional computed tomographic (CT) images before (left) and after (right) adoptive cell transfer. **b**, Regression of a left lung post-operative local recurrence and mediastinal lymph nodes in a patient with metastatic rectal cancer (patient 4378). **c**, Regression of bronchoscopically documented lymphangitic right lung involvement (top, axial orientation), retroperitoneal lymph nodes and perihepatic tumors (middle and bottom, coronal orientation) in a patient with metastatic colon cancer (patient 4420). **d**, Regression of liver metastasis, portal lymph nodes and multiple lung metastases in a patient with metastatic rectal cancer (patient 4405; 'A' indicates a post-ablation artifact).

We also characterized the phenotypes of persistent TCR-transduced cells in post-transfer PBLs (Supplementary Fig. 8). We noticed appreciable patient-to-patient variability, but no parameters appeared to correlate with clinical response.

In patient 4378, we evaluated the function of the persistent TCR-transduced cells by measuring IFNγ secretion by post-transfer PBMC samples in response to peptide-pulsed autologous DCs (Supplementary Fig. 9). In the samples we tested, if TCR-transduced cells were detected, those PBLs specifically secreted IFNγ in response to the relevant mutant peptide compared with the wild-type peptide.

Finally, we measured percentages of $CD4^+FoxP3^+$ cells in PBMCs collected from patients at approximately 1 week and 1 month post-treatment (Supplementary Fig. 10). Although we detected low levels of T regulatory cells in every patient, there was no apparent correlation of the levels of these T cells with clinical response.

Exploratory analyses of post-transfer serum

For every patient, we collected serum at various time points after treatment and measured the levels of IFNγ and IL-2 (Supplementary Fig. 11). Levels of IL-2 appeared to be commensurate with the number of IL-2 doses the patient received as part of their treatment. Serum from patients 4378, 4405, 4469 and 4484 collected 1 or 2 days after therapy contained levels of IFNγ that exceeded 250 pg ml^{-1}, but this did not appear to correlate with clinical responses or toxicities.

As our neoantigen-reactive TCRs contained murine constant regions, we investigated whether these might induce human anti-murine TCR antibodies post-treatment (Supplementary Fig. 12). We identified one patient (4293) who did not respond to therapy and who developed an anti-TCR antibody response, and anti-TCR IgGs were not apparent in serum samples before day 141 post-treatment.

Treatment of patients with retrovirally transduced PBLs expressing neoantigen-reactive TCRs as second-line ACT

During the evolution of our neoantigen TCR clinical trial reported herein, we treated six patients with TCR-transduced PBLs who had previously been treated with adoptively transferred TILs in the context of another trial (ClinicalTrials.gov NCT01174121) (Supplementary Table 3). In addition, we treated a seventh patient who had previously received adoptively transferred PBLs retrovirally transduced to express a murine KRAS(G12D)-reactive TCR generated by vaccinating HLA-A11 transgenic mice in the context of a third trial (ClinicalTrials.gov NCT03745326)[19]. All of these patients had undergone at least two different chemotherapy

https://doi.org/10.1038/s41591-024-03109-0

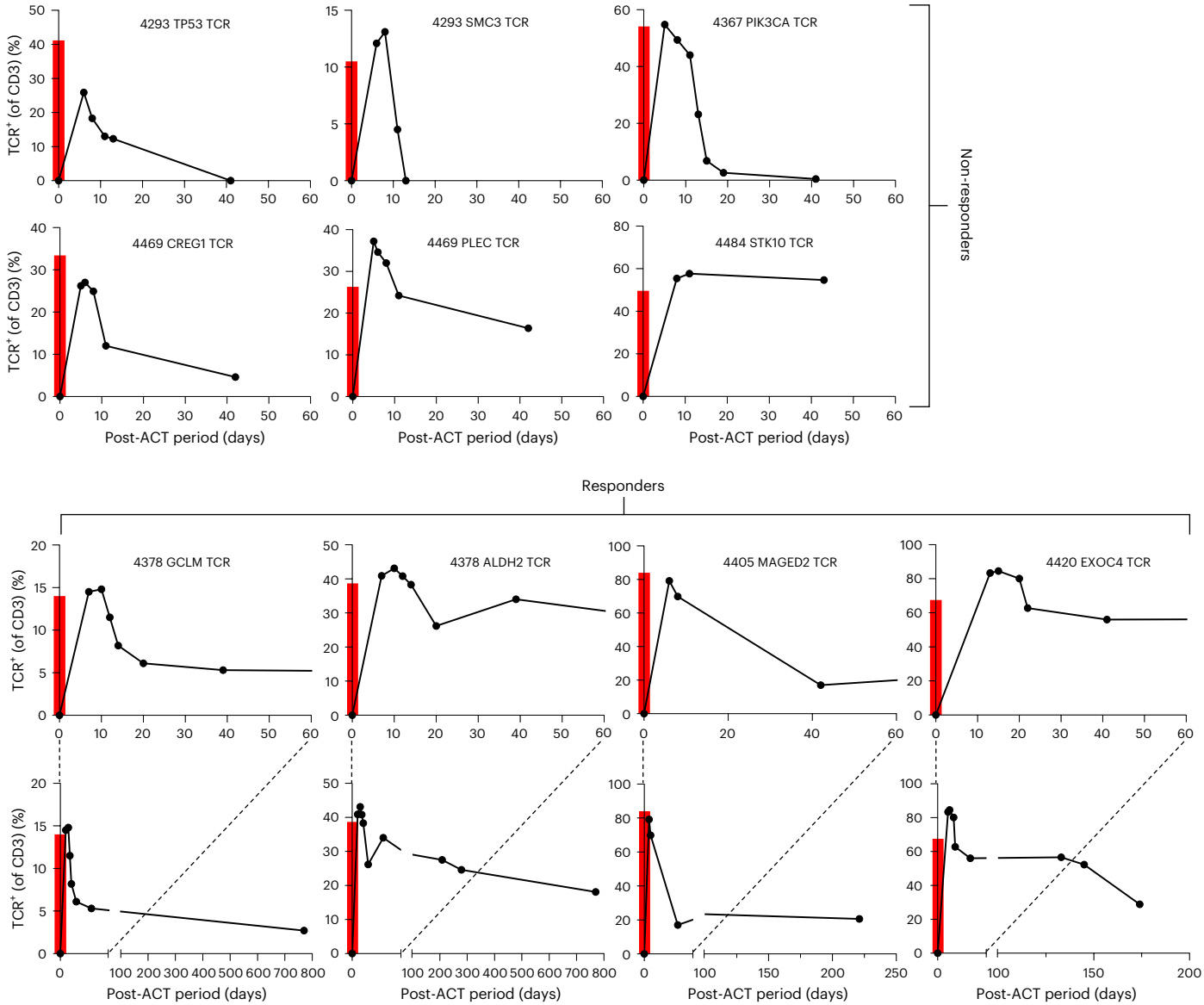

Fig. 4 | Persistence of TCR-transduced cells in PBL. Data for patients who did not respond to therapy are presented in the top 2 rows, and data for the three patients who had partial responses are presented in the bottom 2 rows. As PBLs from later time points were available for the three responders, expanded persistence graphs are shown in the last row for these patients. The red bars at day 0 indicate the percentage of TCR-transduced cells in the patient's final infusion product.

regimens before their first ACT (Supplementary Table 4). None of these patients responded to their primary T cell therapies and were then transitioned to second treatments with individualized neoantigen-reactive TCR-transduced PBLs. None of these patients responded to their TCR treatments (Supplementary Fig. 13), which may be related to the fact that many of the same neoantigens were ineffectively targeted by the previous treatments. For all of these patients, we analyzed their TCR infusion products, their pre- and post-treatment PBL, and their post-treatment serum as we did for the seven T cell treatment-naive patients (Supplementary Figs. 14–21 and Supplementary Tables 5–8).

For these patients, our justification for retreating them with TCR-transduced PBLs was that we might be able to give them products containing more neoantigen-reactive T cells with less differentiated phenotypes. For each patient, we compared the percentages of reactive cells in both T cell products (Extended Data Table 4). For six of these seven patients (all except 4275), we estimated that the number of neoantigen-reactive T cells in the second product was 10 to 100 times greater than the number of reactive cells targeting the same neoantigens in the first treatment (Extended Data Table 4). We also evaluated T cell phenotypes based on CD39 and CD69 expression. For three patients in whom we evaluated bulk TIL products, only 1.6% to 3.2% of all T cells had a less differentiated $CD39^{-}CD69^{-}$ phenotype. In comparison, for the 7 TCR-transduced cell products, these percentages ranged from ~12% to 39% of the actual neoantigen-reactive T cells. Patients treated with TCR-transduced T cells received more cells targeting the same neoantigens against which were able to develop TCRs compared with their first ACT treatments, and those cells had a less differentiated phenotype than routinely observed in TIL cultures.

Because there was a suggestion that TCRs derived from neoantigen-reactive $CD8^{+}$ T cells might be therapeutically beneficial, we performed single-cell RNA-seq on T cells in infused products from 4 patients who received CD8-derived TCRs: 4378 and 4420, who were T cell treatment naive and responded to therapy, and 4275 and 4317 who had previously been treated with TILs (Supplementary Fig. 22). Individual T cells expressing neoantigen-reactive TCRs

were FACS sorted, and unsupervised transcriptomic clustering of TCR-engineered T cells followed by uniform manifold approximation and projection (UMAP) analysis defined $CD8^+$ and $CD4^+$ TCR-engineered T cells in the infusion products (Supplementary Fig. 22a). Sub-setting and specific analysis of the $CD8^+TCR^+$ T cells in the infusion products revealed no single cell state that distinguished cells of patients who responded to therapy (4378 and 4420) from cells of those who did not (4275 and 4317; Supplementary Fig. 22c). Consistent with FACS staining (Extended Data Table 3), the majority of the cells existed in an effector-memory cell state (C0, 53.17% of all $CD8^+$ T cells; Supplementary Fig. 22c).

Discussion

ACT with T lymphocytes genetically modified via retroviral transduction to express personalized neoantigen-reactive TCRs can be tolerated and can mediate tumor regression in some patients with metastatic colorectal cancers refractory to conventional therapies. We treated seven patients who were naive to previous T cell-based therapy, and three of these patients had partial objective clinical responses by RECIST criteria. We believe it is important to report these early findings as the patient responses described here represent proof of principle that an approach using a personalized TCR strategy targeting random somatic mutations may lead to tumor regression, an observation which has never been previously reported.

In a previous clinical study (NCT03970382), 16 patients with different types of refractory solid cancers were treated with autologous PBLs that had been genetically modified using a non-viral precision genome-editing method to express personalized neoantigen-reactive TCRs[20]. No objective clinical responses were observed. That study was conducted as a dose-escalation trial, and the numbers of T cells expressing neoantigen-reactive TCRs given to patients ranged from 2.0×10^8 to 5.4×10^9 with a median of 1.3×10^9 infused neo-TCR^+ cells. In comparison, the range of neoantigen-reactive TCR-transduced cells we administered ranged from 1.8×10^{10} to 1.0×10^{11} with a median of 7.8×10^{10} neo-TCR^+-infused cells. In addition, they only gave low-dose subcutaneous IL-2 to 4 of the 16 patients, whereas all but one patient in our trial received at least one high dose of IL-2 intravenously. These differences may in part explain the enhanced therapeutic efficacy observed in our trial.

We evaluated the phenotypes of the pre-treatment PBLs used for transduction, the function and phenotypes of the adoptively transferred cells, and the persistence of the adoptively transferred cells in the circulation of patients post-treatment, but we did not identify any clear correlates with clinical response. Nonetheless, this study may provide insight about how to improve the therapy. We are currently exploring methods for hastening the TCR identification process. Neoantigen-reactive TCRs can be identified using transcriptomic gene signatures of T cells from fresh tumor digests[7,21] and by FACS sorting $CD8^+$, PD-1^+, $CD39^+$ and $TIGIT^+$ T cells from freshly resected tumors[17]. Both methods bypass the need to expand T cells from TIL fragments before screening. In addition, we have previously identified neoantigen-reactive TCRs using transcriptomic gene signatures of PBLs[22] and by sorting PBLs with neoepitope and HLA tetramers[23]. If sequencing data from primary tumor biopsies are available, we could potentially screen PBLs and identify neoantigen TCRs without the need for additional tumor resections.

Both patients who received TCRs derived from HLA class I-restricted $CD8^+$ T cells had objective clinical responses. We previously observed that only about half of neoantigen reactivities found in TILs from patients with gastrointestinal cancers were HLA class I restricted[1]. However, using gene signatures from both fresh tumor digests and peripheral blood[22], and by FACS sorting specific cells from both sources[23], we have been able to identify CD8-reactive TCRs that were not found in TILs using conventional screening methods. We have also been able to identify novel CD8-derived TCRs through neoantigen-specific in vitro stimulation of T cells derived from peripheral blood and tumors[24]. We are currently pursuing all of these approaches to identify additional CD8-derived TCRs for patients with common epithelial cancers.

Multiple studies in mice and humans suggest that tumor-antigen-specific T lymphocytes with less differentiated phenotypes are positively associated with clinical outcome[6–8,18]. Our protocol for producing large numbers of neoantigen-reactive T cells involves two potent anti-CD3 stimulations that induce cell proliferation and differentiation. We evaluated the phenotypes of TCR-transduced cells immediately before and 2 weeks after the second stimulation, and not surprisingly, we observed that cells were more differentiated after the second stimulation (Supplementary Fig. 23). In addition, there were statistically significant decreases in the overall percentages of TCR-transduced cells. Therefore, we are currently developing methods to expand TCR-transduced cells without performing a second stimulation with anti-CD3.

In a previous study in which patients with melanoma were treated with adoptively transferred TILs, there was a positive correlation between the numbers and percentages of $CD39^-CD69^-$ double-negative cells and response[7]. Interestingly, the adoptively transferred cells given to the two T cell treatment-naive patients who received CD8-derived TCRs had objective clinical responses and contained the highest percentages of $CD39^-CD69^-$ double-negative cells (or $CD39^-$ cells as a single marker) (Extended Data Table 3 and Supplementary Fig. 23). Taken collectively, these observations suggest that sorting or selectively transducing these double-negative cells before therapy may be beneficial.

Tumor cell heterogeneity and HLA LOH present two formidable challenges for developing TCR therapies targeting neoantigens. Five of the neoantigens we targeted in the current study were subclonal, and HLA LOH was found in a resected tumor from one patient (Table 2). In addition, we have previously identified patients treated with neoantigen-reactive T cells who have recurred with tumors with HLA LOH resulting in the specific loss of the MHC restricting element for the targeted neoantigen[25]. Due to complex logistics associated with producing individual GMP-quality retroviruses and T cell products, we currently limit patient treatments to a single product combining up to five individual TCRs, and thus far, we have only treated patients with a maximum of two TCRs. To address tumor cell heterogeneity and HLA LOH, we believe it is critical to treat patients with a diversity of neoantigen-reactive TCRs. To that end, we are currently trying to identify as many TCRs as possible for each patient using gene signatures and in vitro stimulation of PBLs and TILs in addition to our standard TIL screening methodology. Finally, we are developing streamlined retrovirus and cell manufacturing processes that will allow us to target up to ten neoantigens in one final TCR-infusion product, which would make this treatment more practical and potentially overcome tumor heterogeneity and immune resistance.

Online content

Any methods, additional references, Nature Portfolio reporting summaries, source data, extended data, supplementary information, acknowledgements, peer review information; details of author contributions and competing interests; and statements of data and code availability are available at https://doi.org/10.1038/s41591-024-03109-0.

References

1. Parkhurst, M. R. et al. Unique neoantigens arise from somatic mutations in patients with gastrointestinal cancers. *Cancer Discov.* **9**, 1022–1035 (2019).
2. Prickett, T. D. et al. Durable complete response from metastatic melanoma after transfer of autologous T cells recognizing 10 mutated tumor antigens. *Cancer Immunol. Res.* **4**, 669–678 (2016).

3. Stevanovic, S. et al. Landscape of immunogenic tumor antigens in successful immunotherapy of virally induced epithelial cancer. *Science* **356**, 200–205 (2017).
4. Tran, E. et al. Cancer immunotherapy based on mutation-specific CD4+ T cells in a patient with epithelial cancer. *Science* **344**, 641–645 (2014).
5. Zacharakis, N. et al. Breast cancers are immunogenic: immunologic analyses and a phase II pilot clinical trial using mutation-reactive autologous lymphocytes. *J. Clin. Oncol.* **40**, 1741–1754 (2022).
6. Crompton, J. G., Sukumar, M. & Restifo, N. P. Uncoupling T-cell expansion from effector differentiation in cell-based immunotherapy. *Immunol. Rev.* **257**, 264–276 (2014).
7. Krishna, S. et al. Stem-like CD8 T cells mediate response of adoptive cell immunotherapy against human cancer. *Science* **370**, 1328–1334 (2020).
8. Sade-Feldman, M. et al. Defining T cell states associated with response to checkpoint immunotherapy in melanoma. *Cell* **175**, 998–1013.e20 (2018).
9. Morgan, R. A. et al. Cancer regression in patients after transfer of genetically engineered lymphocytes. *Science* **314**, 126–129 (2006).
10. Robbins, P. F. et al. A pilot trial using lymphocytes genetically engineered with an NY-ESO-1-reactive T-cell receptor: long-term follow-up and correlates with response. *Clin. Cancer Res.* **21**, 1019–1027 (2015).
11. Robbins, P. F. et al. Tumor regression in patients with metastatic synovial cell sarcoma and melanoma using genetically engineered lymphocytes reactive with NY-ESO-1. *J. Clin. Oncol.* **29**, 917–924 (2011).
12. Parkhurst, M. R. et al. T cells targeting carcinoembryonic antigen can mediate regression of metastatic colorectal cancer but induce severe transient colitis. *Mol. Ther.* **19**, 620–626 (2011).
13. Linette, G. P. et al. Cardiovascular toxicity and titin cross-reactivity of affinity-enhanced T cells in myeloma and melanoma. *Blood* **122**, 863–871 (2013).
14. Morgan, R. A. et al. Cancer regression and neurological toxicity following anti-MAGE-A3 TCR gene therapy. *J. Immunother.* **36**, 133–151 (2013).
15. Dudley, M. E., Wunderlich, J. R., Shelton, T. E., Even, J. & Rosenberg, S. A. Generation of tumor-infiltrating lymphocyte cultures for use in adoptive transfer therapy for melanoma patients. *J. Immunother.* **26**, 332–342 (2003).
16. Cohen, C. J., Zhao, Y., Zheng, Z., Rosenberg, S. A. & Morgan, R. A. Enhanced antitumor activity of murine–human hybrid T-cell receptor (TCR) in human lymphocytes is associated with improved pairing and TCR/CD3 stability. *Cancer Res.* **66**, 8878–8886 (2006).
17. Chatani, P. D. et al. Cell surface marker-based capture of neoantigen-reactive $CD8^+$ T-cell receptors from metastatic tumor digests. *J. Immunother. Cancer* **11**, e006264 (2023).
18. Rosenberg, S. A. et al. Durable complete responses in heavily pretreated patients with metastatic melanoma using T-cell transfer immunotherapy. *Clin. Cancer Res.* **17**, 4550–4557 (2011).
19. Wang, Q. J. et al. Identification of T-cell receptors targeting KRAS-mutated human tumors. *Cancer Immunol. Res.* **4**, 204–214 (2016).
20. Foy, S. P. et al. Non-viral precision T cell receptor replacement for personalized cell therapy. *Nature* **615**, 687–696 (2023).
21. Hanada, K. I. et al. A phenotypic signature that identifies neoantigen-reactive T cells in fresh human lung cancers. *Cancer Cell* **40**, 479–493 e476 (2022).
22. Yossef, R. et al. Phenotypic signatures of circulating neoantigen-reactive $CD8^+$ T cells in patients with metastatic cancers. *Cancer Cell* **41**, 2154–2165.e5 (2023).
23. Cohen, C. J. et al. Isolation of neoantigen-specific T cells from tumor and peripheral lymphocytes. *J. Clin. Invest.* **125**, 3981–3991 (2015).
24. Cafri, G. et al. Memory T cells targeting oncogenic mutations detected in peripheral blood of epithelial cancer patients. *Nat. Commun.* **10**, 449 (2019).
25. Kim, S. P. et al. Adoptive cellular therapy with autologous tumor-infiltrating lymphocytes and T-cell receptor-engineered T cells targeting common p53 neoantigens in human solid tumors. *Cancer Immunol. Res.* **10**, 932–946 (2022).

Methods

Patient eligibility

All patients had treatment-refractory solid epithelial cancers, were aged 18 years or older and had an Eastern Cooperative Oncology Group performance status ≤1 and no evidence of active major medical diseases. A patient CONSORT diagram is presented in Supplementary Fig. 24.

Inclusion and ethics

These studies were approved by the Institutional Review Board of the National Cancer Institute (NCI). Written informed consent was obtained from all patients, and all studies were conducted in accordance with the International Conference on Harmonization Good Clinical Practice and the applicable portions of the US Code of Federal Regulations. Neither sex nor gender was considered in the study design.

Study design and treatment

All patients were enrolled into an ongoing early phase II pilot study designed to evaluate the safety and efficacy of ACT of autologous PBLs genetically modified via retroviral transduction to express personalized neoantigen-reactive TCRs after non-myeloablative lymphodepleting chemotherapy in patients with metastatic epithelial cancer (ClinicalTrials.gov identifier NCT03412877; https://clinicaltrials.gov/study/NCT03412877?id=NCT03412877&rank=1).

With cell infusion designated as day 0, lymphodepleting chemotherapy consisted of cyclophosphamide (60 mg kg^{-1} once daily) administered on days −7 and −6. Fludarabine (25 mg m^{-2} once daily) was administered from day −7 to day −3. After cell infusion, aldesleukin (IL-2; 720,000 IU kg^{-1}) was given every 8 h to tolerance. The arm of the study reported here included the administration of pembrolizumab 2 days before cell infusion with up to three subsequent doses delivered at 3 week intervals, when clinically appropriate. We previously observed that in vivo expression of PD-1 was increased in adoptively transferred cells modified to express TCRs reactive with tumor-associated antigens when comparing 1 month post-treatment peripheral blood to the initial infusion product[26]. This consideration led to the addition of a pre-cell dose of pembrolizumab to prevent blockade upon infusion. There is no demonstrated clinical efficacy of single agent pembrolizumab in MMR-proficient colorectal cancers, and the drug was given at a time when the patients' immune repertoire has been lymphodepleted. Pembrolizumab was used as an adjunct to the cell transfer regimen, and we expected limited contribution to direct tumor response.

End points

The primary end point of this clinical study was the objective response rate as measured using RECIST 1.1. Cross-sectional imaging was performed pre-treatment, at 6 weeks post-treatment and at regular intervals thereafter until progression. The secondary end points of the study were safety and tolerability. The exploratory end points of the study were the identification of neoantigen-reactive TCRs and the feasibility of manufacturing clinical-grade retroviruses and cell products. There was no prespecified interim analysis defined in this study.

Identification of neoantigens recognized by TILs

WES and RNA-seq on tumor tissue and normal peripheral blood cells were performed by Personal Genome Diagnostics, the Broad Institute and the Surgery Branch, NCI. The data were processed, and variants were called as previously described[1,4]. All genomic NGS data will be deposited in dbGaP in the raw fastq format, and all code used in our analysis will be available for academic use upon request.

TILs were generated from patients by dissecting resected lesions into small fragments and allowing the infiltrating T lymphocytes to migrate out of the fragments and expand individually in vitro in the presence of IL-2 as previously described[15]. All resections and peripheral lymphocyte collections were performed at least 4 weeks after the last dose of cytotoxic chemotherapy or radiation to minimize the potential impact of those treatments on lymphocytes. To determine whether any of the TIL cultures specifically recognized any of the potential neoantigens encoded by mutations present in the autologous tumor(s), we evaluated recognition of autologous DCs transfected with TMGs encoding all the mutations or pulsed with synthetic peptide pools (PPs) containing mutant peptides. For some tumors, particularly those with mutational burdens of 200 or more, screening is limited using filters that account for expression of the variant transcript in RNA-seq and the presence or absence of the variant in multiple tumor samples. TMGs and PPs were constructed as previously described[1,4]. For each single nucleotide variant, we constructed a minigene with the variant nucleotide in the middle flanked on both sides with nucleotides encoding 12 amino acids from the normal protein. For frameshift mutations, we constructed a minigene encoding the variant amino acid sequence until a stop codon was reached. We then concatenated 20 of these minigenes on average into one TMG construct and transcribed RNA in vitro. We also made synthetic 25-amino-acid peptides. Peptides were either made in-house via Fmoc chemistry using ResPep automated tabletop peptide synthesizers (Intavis; CEM) or purchased from Genscript or Thermo Fisher. For single nucleotide variants, the mutant amino acid was placed in the middle and flanked on both sides with 12 amino acids from the normal protein sequence. For frameshift mutations, we made 25-amino-acid peptides, overlapping by 15 amino acids, covering the variant amino acid sequence until a stop codon was reached. We then combined peptides into pools containing 10–24 peptides per pool. Finally, we loaded these TMG RNAs and PPs onto autologous DCs, allowing relevant epitopes to be processed and presented on the cell surface in the context of MHC molecules, such that the DCs acted as an avatar for the patient's tumor cells. Each TIL fragment population that had been expanded in vitro for 2 weeks to 4 weeks with IL-2 was then cocultured with RNA-electroporated and/or peptide-pulsed autologous DCs and evaluated for recognition by measuring IFNγ secretion by ELISPOT and expression of the activation markers 4-1BB and OX40 by FACS.

Identification and construction of potential neoantigen-reactive TCRs

From neoantigen-reactive TIL cultures, we attempted to isolate and characterize the TCRs that mediated recognition as previously described[1,4]. Briefly, individual T cells that upregulated an activation marker (4-1BB or OX40) upon coculture with mutant TMGs or peptides were sorted by FACS. RNA from these cells was isolated, and cDNA was reverse transcribed. cDNA was then sequenced using either a nested PCR with primers specific for the TCR α and β chains or a next-generation sequencing approach[5,27]. Alternatively, for one patient, potential neoantigen-reactive TCRs were identified from FACS-sorted single cells expressing CD8, PD-1, CD39 and TIGIT from a fresh tumor digest as previously described[17]. Construction of potential mutation-reactive TCRs was done by fusing the TCRα V–J regions to the mouse TCRα constant chain, and the TCRβ V–D–J regions to the mouse TCRβ constant chain separated by a furin SGSG P2A linker. Use of mouse TCR constant regions promotes pairing of the introduced TCR and facilitates identification of positively transduced T cells by flow cytometry using an antibody specific for the mouse TCRβ chain constant region (eBioscience).

Evaluation of potential neoantigen-reactive TCRs

TCRs were introduced into autologous or allogeneic PBLs as previously described[1,4]. Briefly, cryopreserved apheresis samples were thawed and stimulated with 50 ng ml^{-1} soluble agonistic anti-CD3 (OKT3; Miltenyi Biotec) and 300–1,200 IU rhu IL-2 (Chiron) for 2 days before retroviral transduction. To generate transient retroviral supernatants, the retroviral vector MSGV1 encoding the potential mutation-reactive TCR and the envelope vector encoding plasmid RD114 were co-transfected into the retroviral packaging cell line 293GP using Lipofectamine 2000

(Life Technologies). Retroviral supernatants were collected ~48 h after transfection, diluted 1:1 with DMEM media containing 10% FCS and then centrifuged onto RetroNectin (Takara Bio)-coated, non-tissue culture-treated plates at 2,000*g* for 2 h at 32 °C. Activated T cells were then spun onto the retrovirus-coated plates for 10 min at 300*g*. GFP and mock transduction controls were included in transduction experiments. Cells were typically assayed 10–14 days post-retroviral transduction for recognition of TMG-electroporated and/or peptide-pulsed autologous DCs by measuring IFNγ secretion by enzyme-linked immunosorbent assay (ELISA) and expression of 4-1BB by FACS.

Mutation clonality analysis

To determine clonality of each mutation (that is, CCF), the local copy number and tumor purity were first determined from WES using Sequenza[28]. Matched normal samples were used as references and hg19 as coordinates. The copy number for a given mutation was calculated by integrating the local copy number, tumor purity and variant allele frequency (VAF)[29]. Only mutations with tumor coverage of at least 20× were used for this analysis. The mutation copy number, tumor purity and VAF were integrated and analyzed using PyClone[30]. In this analysis, all mutations with read depth greater than 4 and VAF greater than 7% were clustered using PyClone v1.3.0 Dirichlet process clustering, which allowed grouping of clonal and subclonal mutations based on their CCF estimates. The mutations were classified as clonal if the 95% confidence interval of their CCF overlapped with 1. Otherwise, they were defined as subclonal. To accomplish this, PyClone was run with 50,000 iterations and a burn-in of 1,000, and the analysis was performed in the R statistical environment, v.3.4.0.

Expression of neoantigens

RNA-seq alignments were performed using the STAR (https://github.com/alexdobin/STAR) two-pass method to human genome build hg19. Duplicates were marked and sorted using Picard's MarkDuplicates tool. Reads were then split and trimmed using the GATK SplitNTrim tool, after which indel realignment and base recalibration were performed using the GATK toolbox. A pileup file was created using the final recalibrated bam file, and variants were called using Varscan2 only. To generate expression quartiles, fragments per kilobase of transcript per million mapped reads (FPKMs) were determined for all genes using Cufflinks[29] under default settings. For each individual patient, all genes with an FPKM value greater than 0 were used to determine quartiles of expressed genes and genes were then assigned to appropriate quartiles. All unexpressed genes were grouped into quartile 1 for that patient.

HLA typing and haplotype-specific copy number analysis of HLA loci

WES data of tumor and germline (peripheral blood) samples for each patient were mapped to the human reference genome (hg19) using Novoalign (Novocraft). The cellularity and purity of these samples were estimated using Sequenza[28]. HLA typing of patients' germline data was computationally determined by taking consensus of predictions from two HLA-typing algorithms, HLA_PRG_LA (ref. 31) and PHLAT (ref. 32). With the patient's HLA typing, cellularity and ploidy estimates, and tumor and germline BAM files, we checked for LOH in the HLA class I alleles using an adjusted version of the original LOHHLA tool[33]. This custom version of the LOHHLA tool is deposited in Bitbucket (https://bitbucket.org/SENTISCI/lohhla/src/master/).

Manufacture and characterization of clinical-grade retroviral supernatants

Retroviral vectors were manufactured using plasmids procured from Genscript. The transfer plasmid containing the individual TCR is an MSGV1 derivative. The TCR and RD114 envelope plasmids were transiently transfected into 293GP cells. The 293GP cell line is a derivative of the 293T line and stably expresses the Moloney murine leukemia virus gag and pol proteins. The cell line was expanded into a Master Cell Bank at the Indiana University Vector Production Facility in compliance with GMP regulations and tested to meet specifications for use in GMP manufacturing: sterility, mycoplasma, adventitious viruses, human viral contaminants, identity and replication-competent retrovirus. A new vial of 293GP cells was thawed for each vector production run and scaled up to at least one ten-layer stack over 10 days in DMEM (Thermo Fisher Scientific) plus 10% FBS (Hyclone). Confluence, cell number and viability were assessed at each split and manipulation as in-process controls. Mixtures of plasmids (~1:1.5 ratio of envelope to transfer vector) and Lipofectamine 2000CD (Thermo Fisher Scientific) were incubated in Opti-MEM Reduced Serum Medium (Thermo Fisher Scientific) according to the manufacturer's recommendations and added to ten-layer stacks containing 293GP cells overnight. The medium was exchanged after 24 h. Benzonase endonuclease (Millipore) was added on the day of collection (day 14) at 50 units ml^{-1} of vector supernatant and incubated for at least 1 h. Following benzonase treatment, the vector supernatant was filtered through a leukocyte reduction filter (Pall Medical) and the product was transferred in 100 g aliquots to freezing bags. Vector supernatants (product and testing samples) were frozen at −80 °C. End-of-production cells were collected, counted, aliquoted and viably frozen per testing plans.

Vector supernatant was tested to meet COA specifications as follows:

Titer and TCR expression: Wells in a 24-well plate were coated with RetroNectin (Takara Bio; 100 μg ml^{-1}) overnight at 4 °C. Plates were blocked with 10% human serum albumin (HSA; Grifols). Vector supernatant was titrated in DMEM plus 10% FBS, added to each well and spun for 2 h at 2,000*g*. Supernatant was aspirated and 2.5×10^5 activated T cells (48 h with 50 ng ml^{-1} OKT3 (Thermo Fisher Scientific); 300 IU ml^{-1} IL-2) were added to each well. FACS analysis was performed 4 days later. Cells were stained with PI (BD Biosciences), phycoerythrin (PE) anti-mouse TCRβ (BD Biosciences) and APC anti-CD3 (Biolegend). Percent positive was reported on live lymphocytes expressing CD3 and murine TCRβ. Titer was calculated by multiplying the percent positive by the number of cells in the well at transduction and the dilution factor to give transducing units per milliliter (TU ml^{-1}). The reported TU ml^{-1} is an average titer of the dilutions that yielded a percent positive between 2% and 30% to capture the majority of cells with one integrated copy. COA specification required ≥30% TCR expression and $\geq 1 \times 10^5$ TU ml^{-1}.

PBL specificity and potency: Autologous APCs (DCs or B cells) or APCs presenting the appropriate HLA complex were pulsed with mutant 25-amino-acid peptides (>95% HPLC purified) or 9–10-amino-acid minimal epitopes (>95% HPLC purified) or wild-type (>95% HPLC purified) counterparts for 2–4 h. Pulsed APCs were cocultured with transduced T cells at a ratio of 1×10^5 effector to 1×10^5 target cells in U-bottom 96-well plate wells overnight. Plates were gently spun and supernatants were transferred to new plates. IFNγ released into the supernatant was measured by ELISA (R&D Systems). COA specification required ≥200 pg ml^{-1} IFNγ released in mutant peptide coculture and 2× background (APC^+ T cells, no peptide).

Sterility: Vector supernatant was tested in the NIH Department of Laboratory Medicine Sterility Service using the BacT/ALERT system (bioMerieux) for aerobic and anaerobic microbial contaminants. In addition, a Sabouraud dextrose agar (Hardy Diagnostics) plate was streaked for augmented detection of fungal contaminants. Mycoplasma was detected using the MycoSEQ Mycoplasma Real-Time PCR kit (Thermo Fisher Scientific). COA specification was no growth detected or negative.

Endotoxin: Endotoxin levels were determined using the *Limulus* amebocyte lysate PYROGENT-5000 detection system (Lonza) with the ELx808 microplate reader (Lonza). The assay was run according to the manufacturer's instructions. COA specification was ≤0.5 endotoxin units per milliliter.

Replication-competent retrovirus: DNA was extracted using the QIAamp DNA Blood Mini Kit (Qiagen). Primers RD114–F2111 5′ ATACGGTCTGGGAGCCTCAA 3′ and RD114–R2211 5′ CTCCAGCAAACGGGCTGATT 3′, and probe RD114–Prob2141 5′ 56-FAM/AT ATTACAA/ZEN/AACCCCAATCAGCTCCTACAGTCC/3IABkFQ 3′ (Integrated DNA Technologies), were mixed with extracted DNA, TaqMan Fast Universal PCR Master Mix (2×) and No AmpErase UNG (Thermo Fisher Scientific), and amplified. Samples measured included vector supernatant and transduced cells to meet the specification of ≤10 copies μl^{-1} (assay limit of detection) or decreasing signal between samples and time points.

Manufacture and testing of TCR-transduced autologous PBLs for treatment

All processes were conducted in a GMP cleanroom in International Standards Organization 7 suites and International Standards Organization 5 biosafety cabinets and executed in accordance with approved batch records with review and oversight by NCI SB Management, Quality Assurance and Quality Control.

Cryopreserved PBLs were thawed and resuspended at 1×10^6 cells ml^{-1} in Roswell Park Memorial Institute (RPMI) media containing 10% human AB serum (BioIVT), 300 IU ml^{-1} rhIL-2 (Proleukin, Clinigen) and 50 ng ml^{-1} OKT3 (Miltenyi Biotech). Cells were distributed to T-175 flasks (100 ml per flask) and incubated at 37 °C for 2 days until the start of the transduction process.

For some samples, PBLs were enriched for CD4 or CD8 cells depending on the identified TCR coreceptor before transduction. Enrichment was performed via negative selection using the CliniMACS system (Miltenyi Biotech) on the day the PBLs were thawed. CD4 cells were enriched by depleting CD8 cells and vice versa. After the PBLs were thawed, up to 4×10^9 of the recovered cells were resuspended in CliniMACS PBS and EDTA buffer containing 0.5% HSA (Grifols). Gamma-Gard (1.3 ml per 200 ml of cells; Baxalta) and either the CD4 or CD8 CliniMACS reagent were added to the cells. The mixture was incubated with rocking for a minimum of 30 min at room temperature (RT). The CliniMACS was set up with the appropriate tubing set and buffers, according to the manufacturer's recommendations. At the end of the labeling process, the CliniMACS selection was run using a Miltenyi optimized program with cells from the positive and negative fractions collected into separate bags with CliniMACS buffer and 0.5% HSA. After the selection, cells from the positive and negative fractions were collected and analyzed by FACS to determine the purity and efficiency of the selection. The enriched fraction was suspended in media with IL-2 (300 IU ml^{-1}) and OKT3 (50 ng ml^{-1}) and seeded into T-175 flasks at 1×10^6 cells ml^{-1} at 100 ml per flask. Cells were incubated at 37 °C until the start of the transduction process.

Before transduction, non-tissue-culture-treated six-well plates were coated with 20 µg per well of RetroNectin (Takara) and incubated for 2 h at RT. Plates were then blocked with 2.5% HSA in PBS for 30 min at RT. The wells were aspirated and washed with HBSS containing 2.5% HEPES. The frozen retroviral vector supernatant was thawed and diluted 1:1 with RPMI containing 10% human AB serum without IL-2. The wash buffer was aspirated from the wells, and 4 ml of 1:1 diluted vector supernatant was placed in each well. The vector-coated plates were centrifuged at 2,000*g* for 2 h at 32 °C. Four of these plates were used immediately for transduction 1 (Td 1), and the remaining four plates were stored overnight at 4 °C for Td 2 the following day.

To transduce the stimulated PBLs, cells were resuspended in RPMI containing 10% human AB serum with 300 IU IL-2 at 0.5×10^6 ml^{-1}. The vector supernatant and media were aspirated from the respective plates, leaving a thin layer of vector supernatant in each well. Then, 4 ml of the resuspended PBLs was added to each well for a total of 2×10^6 cells per well. The four plates for Td 1 were centrifuged at 1,000*g* for 10 min at 32 °C and then incubated overnight at 37 °C. Td 2 was performed the following day using the four vector-coated plates stored at 4 °C. After the Td 2 plates were allowed to come to RT, transduced PBLs from Td 1 were collected, distributed evenly between all wells of the Td 2 plates, centrifuged at 1,000*g* for 10 min at 32 °C and then incubated overnight at 37 °C. The day following Td 2, cells were collected, centrifuged and resuspended in fresh RPMI containing 10% human AB serum with 300 IU ml^{-1} IL-2 for plating in T-175 flasks at 0.5×10^6 cells ml^{-1} in 50–100 ml per flask.

After transduction, cells were maintained in T-175 flasks at 0.7×10^6 to 2×10^6 cells ml^{-1} in RPMI containing 10% human AB serum and 300 IU ml^{-1} IL-2. Seven days later, cells were restimulated using a rapid expansion protocol (REP). To initiate the REP, a 50:50 medium was prepared by mixing equal volumes of RPMI containing 10% human AB serum and AIM V medium and was supplemented with PenStep (Thermo Fisher), IL-2 (3,000 IU ml^{-1}) and OKT3 (50 ng ml^{-1}). Transduced PBLs were seeded into GREX 100 flasks (WilsonWolf) at 5×10^6 cells per flask with irradiated (6,000 rad) donor feeder PBLs at 5×10^8 for a 1:100 ratio. Approximately 1 week after the start of the REP, each GREX 100 flask was split to a cell density of $0.5–2.0 \times 10^6$ cells ml^{-1} with AIM V medium containing GlutaMAX (2 mM; Thermo), Penstrep (Thermo) and IL-2 (3,000 IU ml^{-1}). The cells were maintained with this medium for an additional 7 days at which point the cells were pooled and collected for final formulation and release for infusion.

Cells were sampled for release testing criteria in accordance with the COA at various stages of the manufacturing process.

Endotoxin testing (≤5 endotoxin units per kilogram) and Gram stain (negative) were performed on the morning of cell collection, before final formulation. Cell counts for the final product (that is, infusion bag) were required to be within 1×10^9 to 1.5×10^{11} total cells with >70% viability. Additional samples were taken from the infusion bag for post-manufacturing testing, including final product sterility, replication-competent retrovirus (S+L−), residual benzonase, residual plasmid DNA and vector copy number, but were not required for product release and infusion.

The vector copy number in cell products given to patients was estimated from extracted DNA using the QIAamp DNA Blood Mini Kit (Qiagen). Two separate qPCRs were executed to quantify long terminal repeat (LTR) copies from the MSGV1 vector and albumin gene copies as an endogenous housekeeping gene. As two LTRs are expected per integrant and two albumin gene copies are expected per cell, LTR copies divided by albumin gene copies yielded an average vector copy number per cell across a cell population. Extracted DNA was mixed with TaqMan Fast Universal PCR Master Mix (2×), No AmpErase UNG (Thermo Fisher Scientific) and LTR primers and probe (MSGV-LTR3-F 5′ CAAGGCATGGAAAATACATAACTG 3′, MSGV-LTR3-R 5′ GCTTACCACAGATATCCTGTTTGG 3′, MSGV-LTR3-Prb 5′ 56-FAM/TATTCTGCT/ZEN/GTCTCTCTGTTCCTAACCTTGATCTG/3IABkFQ 3′) or albumin primers and probe (ALB-F 5′ GCTGTCATCTCTTGTGGGCTGT 3′, ALB-R 5′ ACTCATGGG AGCTGCTGGTTC 3′, ALB-Prb 5′ 56-FAM/CCTGTCATG/ZEN/CCCACACAAATCTCCC/ 3IABkFQ 3′; Integrated DNA Technologies) and amplified.

Phenotypic evaluation of PBLs and TCR-transduced cells

We analyzed pre-treatment PBLs, TCR-transduced cells and post-treatment PBLs by FACS using fluorescently labeled antibodies against human CD3 (clone SK7), CD4 (clone SK3), CD8 (clone RPA-T8), CD45RO (clone UCHL1), CD62L (clone DREG-56), CD27 (clone M-T271), CD39 (clone A1) and CD69 (clone FN50), and against murine TCRβ chain (clone H57-597; BD Biosciences) using the manufacturers' recommended dilutions. Flow cytometry data were collected using BD FACSDiva and analyzed with FlowJo. For analyses of PBLs, cryopreserved samples were thawed and rested overnight in the absence of IL-2 before FACS. For analyses of TCR-transduced cells, cryopreserved samples were thawed and rested overnight in the presence of 600 IU ml^{-1} IL-2 before FACS. For patients who received two TCRs, we attempted to identify commercially available antibodies against human Vβ regions that would enable us to distinguish the two. The following antibodies

against specific Vβ regions used by the indicated TCRs were purchased from Beckman Coulter: 4275 GPATCH8 (TRBV4-1, anti Vβ7.1), 4293 TP53 (TRBV5-1, anti Vβ5.1), 4271 CHD2 and 4469 CREG1 (TRBV3-1, anti Vβ9.1), 4378 ALDH2 (TRBV20-1, anti Vβ2) and 4317 APC (TRBV27, anti Vβ14). For the Vβ9.1 and anti Vβ5.1 antibodies, we discovered considerable interference between the Vβ antibody and the murine TCRβ antibody. In particular, the murine TCRβ antibody inhibited the binding of the Vβ antibody under all conditions we tested (antibody titrations and staining with the Vβ antibody before the murine TCRβ antibody). Therefore, to estimate frequencies of persistent TCR-transduced cells for patients 4293, 4271 and 4469, we stained samples with each antibody independently. For the specific Vβ TCRs (4293 TP53, 4271 CHD2 and 4469 CREG1), we estimated the percentages of TCR-transduced cells in PBLs by subtracting endogenous Vβ expression (estimated from pre-treatment PBL) from total Vβ expression in singly stained samples. For the non-Vβ-specific TCRs (4293 SMC3, 4271 USP47 and 4469 PLEC), we estimated the percentages of TCR-transduced cells in PBLs by subtracting the estimated specific Vβ TCR percentages from murine TCRβ expression in singly stained samples. However, due to these interferences, we could not reliably evaluate other phenotypic markers on individual TCR-transduced cells in post-ACT PBLs for these patients.

We evaluated the percentages of T regulatory cells in post-treatment PBLs using anti-human FoxP3 (clone 259D/C7) and anti-human CD4 (clone RPA-T4) (BD Biosciences) using the manufacturer's recommended dilutions. As FoxP3 is an intracellular transcription factor, cells were permeabilized before staining using the BD Pharmingen Transcription Factor Buffer Set according to the manufacturer's instructions.

Functional evaluation of TCR-transduced cells

Cells that were adoptively transferred into patients were functionally evaluated by measuring cytokines and chemokines in supernatants from cocultures of the T cells with peptide-pulsed autologous DCs. For analyses of PBLs, cryopreserved samples were thawed and rested overnight in the presence or absence of IL-2 before functional testing. For analyses of TCR-transduced cells, cryopreserved samples were thawed and rested overnight in the presence of 600 IU ml^{-1} IL-2 before testing, but cells were cocultured in the absence of any exogenous IL-2. IFNγ secretion was measured by ELISA using paired antibodies from Invitrogen: primary anti-human IFNγ monoclonal antibody (clone 2G1: M700A) and biotin-labeled anti-human IFNγ (clone B133.5: M701B) using the manufacturer's recommended dilutions. Secretion of other cytokines and chemokines was measured using FACS-based kits from Miltenyi Biotech (MACSPlex Cytotoxic T/NK Cell Kit, human and MACSPlex Cytokine 12 Kit, human) according to the manufacturer's instructions.

We previously noticed that reactive cells in PBLs are not highly functional in vitro directly upon thawing without any external stimuli[34]. Therefore, in these experiments, we thawed cryopreserved PBMCs and incubated them overnight at 37 °C in the presence or absence of IL-2 before coculture. In the samples we tested, if TCR-transduced cells were detected, those PBLs specifically secreted IFNγ in response to the relevant mutant peptide compared with the wild-type peptide, and the reactivities were slightly enhanced after overnight incubation with IL-2, but this also tended to cause an increase in the background level of IFNγ secretion.

Evaluation of serum cytokines

Levels of IFNγ and IL-2 were measured in patient serum samples using commercially available ELISA kits (Invitrogen).

Evaluation of anti-TCR antibody responses

TCR-transduced cells were incubated with the pre- and post-treatment sera, and the presence of serum antibody binding to TCR-transduced PBLs was determined by FACS using fluorescently labeled anti-human IgG. As a positive control, we included serum samples from a patient treated with a murine NY-ESO-1-reactive TCR (Supplementary Fig. 12a).

Estimation of percentages of neoantigen-reactive T cells in TIL products

In the selected TIL products first given to patients 4217, 4271, 4275, 4285, 4317 and 4414, we estimated the percentages of reactive cells based on TCR β chain sequencing from genomic DNA performed by Adaptive Biotechnologies.

Single-cell RNA analyses

Single-cell transcriptome analyses were performed using QC passed single-cell data for the four TCR-infusion products targeting CD8-neoantigens: 4378 (two TCR-engineered cell products isolated by FACS sorting), 4420, 4275 and 4317. Cells were normalized using the Seurat SCTransform function and then integrated using Seurat's IntegrateData function, followed by PCA function to establish UMAP coordinates, neighbors and clusters. We excluded all TRAV/TRBV genes to remove endogenous TCR expression as a source of clustering bias before processing by Seurat. Initial cell UMAP at a resolution of 1.2 consisted of 20731T cells. CD8-transcriprome expressing T cells were then sub-setted and re-clustered at a resolution of 1 to obtain 8,350 $CD8^+$ T cells with 13 clusters. Cluster-specific markers were identified using the FindAllMarkers function in Seurat with min.pct and log2fc threshold set to 0.25.

Statistical analyses

This trial was designed to evaluate each histologic cohort in a Simon optimal two-stage design to rule out an unacceptably low rate of objective response. For participants treated on arm 2, in each of these four cohorts evaluated individually, the primary objective of the study would be to determine whether using autologous T cells would rule out a 10% response rate and target a rate of 25%. As such, the trial will be conducted using a Simon optimal two-stage phase II trial design to rule out an unacceptably low PR + CR rate of 10% (p0 = 0.10) in favor of an improved response rate of 25% (p1 = 0.25). With alpha = 0.10 (probability of accepting a poor treatment = 0.10) and beta = 0.10 (probability of rejecting a good treatment = 0.10), this first stage will enroll 21 evaluable participants in a given cohort, and if 0–2 of the 21 participants have a clinical response, then no further participants will be accrued in that cohort. If 3 or more of the first 21 evaluable participants in a cohort have a response, then accrual would continue until a total of 50 evaluable participants have been treated. As it may take up to several months to determine whether a participant has experienced a response, a temporary pause in the accrual may be necessary to ensure that enrollment to the second stage is warranted. If there are 3–7 participants with a response out of 50 participants in a cohort, this would be an uninterestingly low response rate. If there are 8 or more of 50 participants (16%) who experience a response, this would be sufficiently interesting to warrant further study in that histology in later trials. Under the null hypothesis (10% response rate), the probability of early termination for a given cohort is 64.8%. With the identification of three objective responses in the patient group reported herein, the strategy has reached the prespecified requirement for continued accrual.

To compare Cmax values between patients who responded to therapy and those who did not, we used an unpaired *T*-test. To compare cell phenotypes before and after in vitro stimulation, we paired *T*-tests. We used GraphPad Prism to perform these calculations. *P* values were considered significant if they were less than 0.05.

Reporting summary

Further information on research design is available in the Nature Portfolio Reporting Summary linked to this article.

Data availability

Next-generation sequencing data for all samples in this study have been deposited in raw fastq format to dbGaP under the study accession phs001003.

Code availability

All code used in this study is available from the corresponding author upon request for academic use. Upon request, the corresponding author will respond within 2 weeks and provide the requested code.

References

26. Abate-Daga, D. et al. Expression profiling of TCR-engineered T cells demonstrates overexpression of multiple inhibitory receptors in persisting lymphocytes. *Blood* **122**, 1399–1410 (2013).
27. Pasetto, A. et al. Tumor- and neoantigen-reactive T-cell receptors can be identified based on their frequency in fresh tumor. *Cancer Immunol. Res.* **4**, 734–743 (2016).
28. Favero, F. et al. Sequenza: allele-specific copy number and mutation profiles from tumor sequencing data. *Ann. Oncol.* **26**, 64–70 (2015).
29. McGranahan, N. et al. Clonal neoantigens elicit T cell immunoreactivity and sensitivity to immune checkpoint blockade. *Science* **351**, 1463–1469 (2016).
30. Roth, A. et al. PyClone: statistical inference of clonal population structure in cancer. *Nat. Methods* **11**, 396–398 (2014).
31. Dilthey, A. T. et al. HLA*LA–HLA typing from linearly projected graph alignments. *Bioinformatics* **35**, 4394–4396 (2019).
32. Bai, Y., Wang, D. & Fury, W. PHLAT: inference of high-resolution HLA types from RNA and whole exome sequencing. *Methods Mol. Biol.* **1802**, 193–201 (2018).
33. McGranahan, N. et al. Allele-specific HLA loss and immune escape in lung cancer evolution. *Cell* **171**, 1259–1271.e11 (2017).
34. Rosenberg, S. A. et al. Immunologic and therapeutic evaluation of a synthetic peptide vaccine for the treatment of patients with metastatic melanoma. *Nat. Med.* **4**, 321–327 (1998).

Acknowledgements

We acknowledge the following people for significant contributions: for WES and RNA-seq analyses, S. Chatmon and T. Benzine; for peptide synthesis, S. Kivitz and M. Florentin; for TCR sequencing, B. Paria and V. Hill; for retroviral vector production, S. Feldman, A. Cuenca, A. Mason, N. Gill, Q. Richburg and T. Novsak; for T cell product production, R. Somerville, Z. Franco, L. Parker, A. Nahvi, M. Langhan, T. Shelton, H. Xu, N. Torres, F. Cobarde and X. Zhao; for quality control, R. Hurst, E. Pool, J. Lowe, A. Nguyen, C. Toy, A. Afzal and P. Chapman; for regulatory affairs, M. Toomey and J. Pappas; for patient care, R. Sherry, L. McIntyre, S. Seitter, A. Choi, A. Gustafson, A. El-Saadi, A. Dinerman, M. Dawson and K. Borkowski. The authors received no specific funding for this work.

Author contributions

M.P., S.L.G., F.J.L., P.F.R. and S.A.R. conceived of and designed the study. M.P., S.L.G., F.J.L., R.K.B., H.H., P.F.R., T.D.P., J.J.G., S.S., S.K., N.Z., N.L., S.P.K. and S.A.R. developed the methodology. M.P., S.L.G., F.J.L., R.K.B., H.H., P.F.R., T.D.P., J.J.G., S.S., L.N., S.R., A.B., R.S., N.L., S.P.K., A.C., S.N., S.L., N.P. and S.A.R. acquired the data (acquired and managed patients, provided facilities and so on). M.P., S.L.G., F.J.L., P.F.R., T.D.P., J.J.G., S.S., J.C.Y. and S.A.R. analyzed and interpreted the data (for example, statistical analysis, biostatistics, computational analysis). M.P., S.L.G., F.J.L., R.K.B., H.H., P.F.R., J.J.G., S.S. and S.A.R. wrote, reviewed and revised the paper. S.L.G., A.C., S.N., S.L., N.P., M.L.M.K., N.D.K., J.C.Y. and S.A.R. were responsible for the clinical care of patients.

Competing interests

The authors declare no competing interests.

Additional information

Extended data is available for this paper at https://doi.org/10.1038/s41591-024-03109-0.

Supplementary information The online version contains supplementary material available at https://doi.org/10.1038/s41591-024-03109-0.

Correspondence and requests for materials should be addressed to Maria Parkhurst.

Peer review information *Nature Medicine* thanks George Coukos and the other, anonymous, reviewer(s) for their contribution to the peer review of this work. Primary Handling Editor: Ulrike Harjes, in collaboration with the *Nature Medicine* team.

https://doi.org/10.1038/s41591-024-03109-0

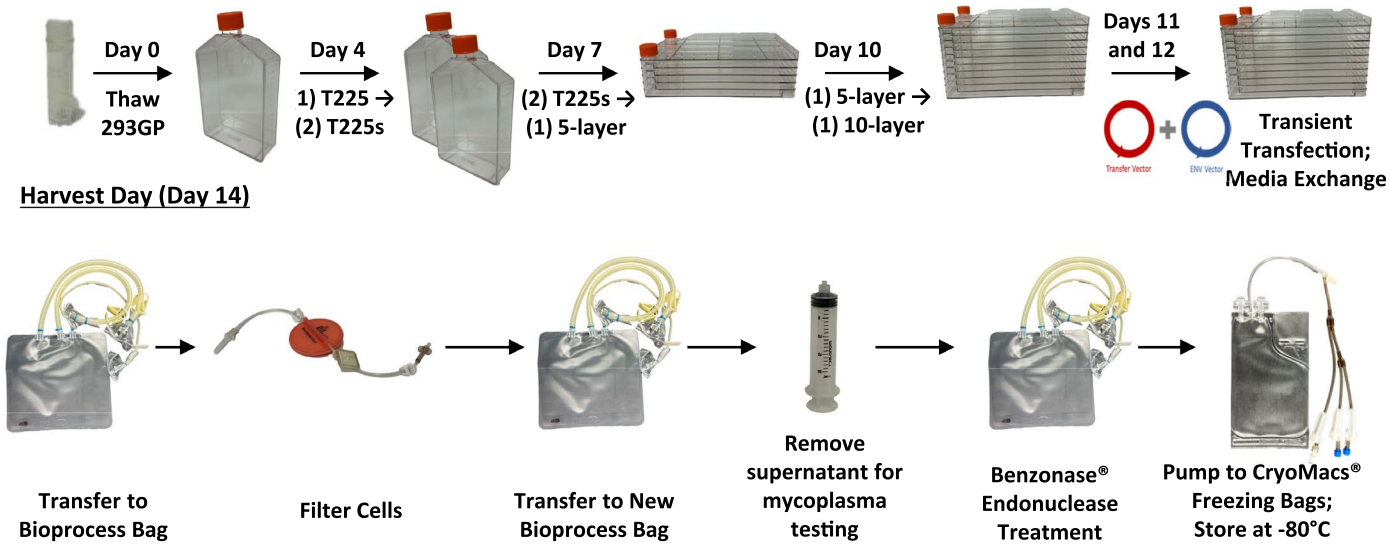

Extended Data Fig. 1 | Manufacture of clinical grade retroviral products. Schematic diagram of our GLP process to generate retroviral products to transduce PBL for patient treatment using transiently transfected 293GP cells.

https://doi.org/10.1038/s41591-024-03109-0

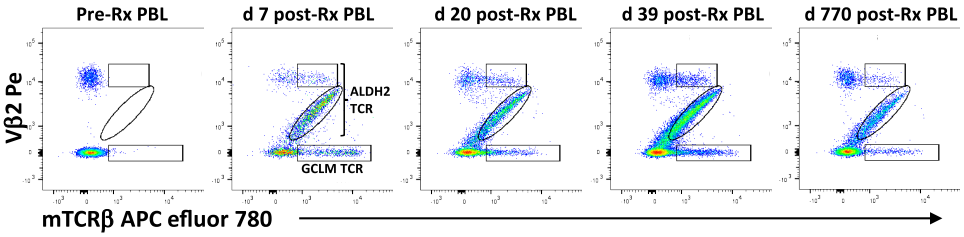

Extended Data Fig. 2 | FACS strategy for evaluating persistence of TCR transduced cells in PBL. Examples of FACs gating strategies to define persistence of GCLM and ALDH2 TCR transduced T cells in post-treatment PBL from patient 4378. Cryopreserved samples from the indicated days pre- and post-ACT were thawed and rested overnight without IL-2 prior to FACS. Cells were stained with antibodies against human CD3, murine TCRβ chain which stained all transduced cells, and human Vβ2 which stained the ALDH2 TCR. Analyses shown were performed on lymphocyte-size gated, live (PI negative), CD3+ T cells. The human Vβ2+ TCRβ- cells represent the endogenous Vβ2 repertoire in the patient's PBL.

https://doi.org/10.1038/s41591-024-03109-0

Extended Data Table 1 | TCR identification

Resection #	total # of variants	# of variants screened	# of TIL screened	Neoantigens identified	CD4/8	TCR used for Rx	HLA restriction element	Minimal epitope	TRAV	CDR3 alpha	TRBV	CDR3 beta
4293	112	53*	11	TP53 (Y236S)	CD4	yes	DRB3*02:01	not determined	TRAV12	CAIGEGNTPLVF	TRBV5-1	CASSTRQGSGGELF
				SMC3 (S900delinsSM)	CD4	yes	not determined	not determined	TRAV29	CAASGYGTGRRALTF	TRBV7-7	CASSLGGVSTDTQYF
				CYP2C9 (F423S)	CD4	no**						
4367	91	91	13	PIK3CA (N345K)	CD4	yes	DPB1*04:01/DPA1*01:03	not determined	TRAV8-04	CAVSEGSGSGSRLTF	TRBV10-1	CASSDRGETGELFF
4378	125	125	24	GCLM (D177N)	CD8	yes	A*25:01	CVMPPNLTAF	TRAV2	CAVDEEAGTALIF	TRBV7-9	CASRSGLAGYNEQFF
				ALDH2 (P184L)	CD8	yes	A*02:01	ILWNFPLLM	TRAV41	CAVTPNTGNQFYF	TRBV20-1	CSATLMGYEQYF
4405	194	194	24	MAGED2 (K150E)	CD4	yes	not determined	not determined	TRAV41	CAVNDYKLSF	TRBV7-2	CASSLDLADEQFF
4420	70	70	6***	EXOC4 (K91N)	CD8	yes	B*35:01	DPLNILANADTM	TRAV29/DV5	CAANPWGNQFYF	TRBV27	CASRPRVATGSPLHF
4469	41	41	21	CREG1 (D67H)	CD4	yes	not determined	not determined	TRAV38-2/DV8	CAYRKNYGGATNKLIF	TRBV3-1	CASSQDSSISPQHF
				PLEC (E4174K)	CD4	yes	not determined	not determined	TRAV12-2	CAGSGGYQKVTF	TRBV7-2	CASSSSTGHTEAFF
4484	143	143	23	STK10 (R867L)	CD4	yes	not determined	not determined	TRAV6	CARQKRNTGFQKLVF	TRBV6-1	CASRDRVGTEAFF

* Screening was limited using filters that accounted for expression of the variant transcript in RNA-seq and the presence or absence of the variant in multiple tumor samples.
** Although we identified CYP2C9 reactivity in TIL fragment cultures, we were unable to isolate a TCR.
*** For this patient, 6 TCRs identified by sorting CD39+ TIGIT+ PD-1+ cells from fresh tumor digests were screened for neoantigen reactivity.

https://doi.org/10.1038/s41591-024-03109-0

Extended Data Table 2 | Characterization of clinical grade supernatants

Resection #	TCR	% mTCRβ+	Titer (units/ml)	Peptide*	IFNγ (pg/ml)		
					Concentration	mutant	wild type
4293	TP53 (Y236S)	54%	2.1E+06	LP	10 µg/ml	496	22.5
	SMC3 (S900delinsSM)	43%	1.0E+06	LP	10 µg/ml	2006	Below Detection
4367	PIK3CA (N345K)	31%	1.7E+05	LP	10 µg/ml	25814	59
4378	GCLM (D177N)	53%	5.7E+05	Min	10 µg/ml	3276	Below Detection
	ALDH2 (P184L)	55%	4.6E+05	Min	1 µg/ml	8001	14
4405	MAGED2 (K150E)	49%	3.4E+05	LP	10 µg/ml	8330	16
4420	EXOC4 (K91N)	64%	1.4E+06	LP	10 µg/ml	289	14
4469	CREG1 (D67H)	70%	1.9E+06	LP	10 µg/ml	5397	43
	PLEC (E4174K)	64%	1.5E+06	LP	1 µg/ml	5105	224
4484	STK10 (R867L)	76%	1.6E+06	LP	1 µg/ml	5553	Below Detection

* LP: long peptides are 25mers; Min.: minimals are those listed in Table 2

https://doi.org/10.1038/s41591-024-03109-0

Extended Data Table 3 | Phenotypic characterization of infused cell products

					Gated on CD3+ mTCRβ+ cells								
Resection #	Neoantigen	Coreceptor selection	# of cells given	Vector copy #	% TCR+	% CD8+	% CD4+	% N	% CM	% EM	% EMRA	% CD39- CD69-	% CD27+
4293	TP53 (Y236S)	no	7.8E+10	1.7	79.6	8.0	91.5	0.5	24.9	73.5	1.1	34.3	3.7
	SMC3 (S900delinsSM)	no	7.2E+10	1.4	21.7	25.6	72.8	4.1	32.0	58.5	5.4	34.4	11.0
4367	PIK3CA (N345K)	yes	1.5E+11	1.2	54.1	0.0	99.2	0.7	18.2	80.1	1.0	37.2	2.8
4378	GCLM (D177N)	no	3.9E+10	1.9	54.1	27.8	47.6	1.0	6.6	87.6	4.8	57.9	14.7
	ALDH2 (P184L)	no	1.1E+11	2.5	52.2	24.2	73.0	0.1	2.1	97.1	0.7	67.0	4.0
4405	MAGED2 (K150E)	yes	1.1E+11	3.0	84.0	0.0	99.4	0.2	18.6	80.9	0.3	31.1	2.1
4420	EXOC4 (K91N)	yes	1.2E+11	2.1	67.5	93.9	0.1	0.1	15.0	84.6	0.3	75.8	25.3
4469	CREG1 (D67H)	no	3.0E+10	2.3	66.7	51.9	42.5	1.1	11.2	86.4	1.4	48.3	8.8
	PLEC (E4174K)	no	3.0E+10	1.7	52.5	54.7	39.1	15.0	10.8	55.2	19.0	38.7	33.0
4484	STK10 (R867L)	no	1.1E+11	1.5	49.6	59.3	35.3	4.2	7.2	79.1	9.5	10.8	20.7

https://doi.org/10.1038/s41591-024-03109-0

Extended Data Table 4 | Comparison of T cell products in patients treated twice with ACT

		1st T cell therapy*				2nd TCR therapy			
Resection #	Neoantigen	Total # of cells infused*	~% reactive cells**	~# of reactive cells infused	%CD39-CD69-	Total # of cells infused	~% reactive cells	~# of reactive cells infused	%CD39-CD69- (of mTCRβ+ cells)
4217	MAP3K2 (S153F)	9.1E+10	1.0	9.1E+08	not tested	5.9E+10	33.1	2.0E+10	33.9
	UEVLD (F191V)		1.2	1.1E+09			33.6	2.0E+10	38.8
	MUC4 (R4435S)		10.5	9.6E+09			not included	not included	
	RAD51B (L321R)		5.6	5.1E+09			not included	not included	
4271	USP47 (F1156L)	5.3E+10	1.6	8.5E+08	not tested	3.1E+10	27.6	8.6E+09	19.1
	CHD2 (K1351R)		1.2	6.4E+08			28.9	9.0E+09	25.9
	WDFY1 (E44K)		0.1	5.3E+07			not included	not included	
	CPSF6 (G178E)		5.0	2.7E+09			not included	not included	
	DHTKD1 (V643I)		13.8	7.3E+09			not included	not included	
4275	GPATCH8 (R954H)	9.6E+10	24.2	2.3E+10	1.8	1.5E+11	27.4	4.1E+10	25.3
	WLS (R445G)		58.5	5.6E+10			36.0	5.4E+10	27.6
4285	TP53 (R175H)	7.0E+10	4.2	2.9E+09	1.6	8.6E+10	29.6	2.5E+10	30.9
	ATP6VOB(Y88F)		2.4	1.7E+09			not included	not included	
4317	PIK3CA (P449T)	3.6E+10	32.9	1.2E+10	3.2	1.5E+11	35.4	5.3E+10	11.9
	APC (E1335fs)		17.1	6.2E+09			34.0	5.1E+10	21.3
	FIZ1(R394W)		4.8	1.7E+09			not included	not included	
4373*	KRAS (G12D)	3.0E+08	49**	1.5E+08	not tested	8.8E+10	72.4	6.3E+10	36.6
4414	TP53(Y220D)	9.0E+10	56.5	5.1E+10	not tested	7.5E+10	not included	not included	
	PPAP2C (L72V)		0.3	2.7E+08			80.0	6.0E+10	20.2

* All patients were previously treated with selected TIL fragments except for 4373 who previously received ACT with autologous PBL retrovirally transduced to express an HLA-A11 restricted KRAS(G12D) reactive TCR derived from HLA-A11 transgenic mice.

** For all TIL products, the percent of reactive cells in TIL infusion samples was estimated based on TCR β chain sequencing performed by Adaptive Biotechnologies.
For 4373, we estimated that 49% of cells in the original T cell product recognized mutant KRAS based on FACS staining with an antibody against the murine TCRb chain constant region.

nature portfolio

Corresponding author(s): Maria Parkhurst

Last updated by author(s): May 22, 2024

Reporting Summary

Nature Portfolio wishes to improve the reproducibility of the work that we publish. This form provides structure for consistency and transparency in reporting. For further information on Nature Portfolio policies, see our Editorial Policies and the Editorial Policy Checklist.

Statistics

For all statistical analyses, confirm that the following items are present in the figure legend, table legend, main text, or Methods section.

n/a	Confirmed
☐	☒ The exact sample size (*n*) for each experimental group/condition, given as a discrete number and unit of measurement
☒	☐ A statement on whether measurements were taken from distinct samples or whether the same sample was measured repeatedly
☐	☒ The statistical test(s) used AND whether they are one- or two-sided *Only common tests should be described solely by name; describe more complex techniques in the Methods section.*
☒	☐ A description of all covariates tested
☒	☐ A description of any assumptions or corrections, such as tests of normality and adjustment for multiple comparisons
☐	☒ A full description of the statistical parameters including central tendency (e.g. means) or other basic estimates (e.g. regression coefficient) AND variation (e.g. standard deviation) or associated estimates of uncertainty (e.g. confidence intervals)
☐	☒ For null hypothesis testing, the test statistic (e.g. *F*, *t*, *r*) with confidence intervals, effect sizes, degrees of freedom and *P* value noted *Give P values as exact values whenever suitable.*
☒	☐ For Bayesian analysis, information on the choice of priors and Markov chain Monte Carlo settings
☒	☐ For hierarchical and complex designs, identification of the appropriate level for tests and full reporting of outcomes
☒	☐ Estimates of effect sizes (e.g. Cohen's *d*, Pearson's *r*), indicating how they were calculated

Our web collection on statistics for biologists contains articles on many of the points above.

Software and code

Policy information about availability of computer code

Data collection	Flow cytometry data was collected using BD FACSDiva and analyzed with FlowJo V10.
Data analysis	Statistical analyses: GraphPad Prism; Variant Callers: Varscan2.3.6, MuTect1.1.7, strelka1.0.15, somaticsniper1.0.5; Alignment: novocraft4.03.05, STAR2.5.4a; DataProcessing: GATK3.4-0, samtools0.1.18, picard1-127; Annotation: Annovar (downloaded April 2019); Expression: Cufflinks2.2.1; BindingPredictions: MHCFlurry1.6, netMHCpan4.0, netMHCIIpan3.1, neMHCstabpan-1.0, netCHOP-3.1; LOHHLA tool: https://bitbucket.org/SENTISCI/lohhla/src/master/

For manuscripts utilizing custom algorithms or software that are central to the research but not yet described in published literature, software must be made available to editors and reviewers. We strongly encourage code deposition in a community repository (e.g. GitHub). See the Nature Portfolio guidelines for submitting code & software for further information.

Data

Policy information about availability of data

All manuscripts must include a data availability statement. This statement should provide the following information, where applicable:

- Accession codes, unique identifiers, or web links for publicly available datasets
- A description of any restrictions on data availability
- For clinical datasets or third party data, please ensure that the statement adheres to our policy

Next Generation sequencing data for all samples in this study has been deposited in its raw fastq format to dbGaP under the study accession phs001003.

Human research participants

Policy information about studies involving human research participants and Sex and Gender in Research.

Reporting on sex and gender	Gender is reported for individual patients based on self-reporting. The immunologic findings are not sex or gender-specific. Consent for research publication is included within the protocol consent and documented with informed consent of participants.
Population characteristics	individual-level data is provided in material and supplemental materials. Median age is 47.8 (IQR 41-51.3). Of the 14 reported patients, 4 patients are self-identified female, the remaining 10 are male. Two patients identified as Asian; the remaining patients identified as White. All patients had measurable and evaluable treatment-refractory metastatic gastrointestinal cancer with a median of 4 prior chemotherapy regimens (IQR 3-6). All patients had an ECOG performance status of 0 or 1.
Recruitment	Patients were recruited using materials and methods approved by the Institutional Review Board. Potential participants were self-referred or referred by their home oncologist and evaluated for a minimal-risk resection of metastatic disease. Bridging therapy was at the direction of the home oncologists while patient biospecimens were analyzed for T-cell receptor discovery and manufacture. There is potential self-selection for patients with metastatic cancer with socioeconomic support for a 3-4 week inpatient hospitalization, as required for the safe administration of the experimental regimen. There also exists a survival bias in that participants had to remain eligible during bridging therapy.
Ethics oversight	The NIH IRB and FDA approved the study protocol.

Note that full information on the approval of the study protocol must also be provided in the manuscript.

Field-specific reporting

Please select the one below that is the best fit for your research. If you are not sure, read the appropriate sections before making your selection.

☒ Life sciences ☐ Behavioural & social sciences ☐ Ecological, evolutionary & environmental sciences

For a reference copy of the document with all sections, see nature.com/documents/nr-reporting-summary-flat.pdf

Life sciences study design

All studies must disclose on these points even when the disclosure is negative.

Sample size	This manuscript contains pilot information on the expected enrollment. The overall trial design is as follows: Simon optimal two-stage phase II trial design in order to rule out an unacceptably low PR+CR rate of 10% (p0=0.10) in favor of an improved response rate of 25% (p1=0.25). With alpha=0.10 (probability of accepting a poor treatment=0.10) and beta = 0.10 (probability of rejecting a good treatment=0.10), this first stage will enroll 21 evaluable participants in a given cohort, and if 0-2 of the 21 participants have a clinical response, then no further participants will be accrued in that cohort. If 3 or more of the first 21 evaluable participants in a cohort have a response, then accrual would continue until a total of 50 evaluable participants have been treated.
Data exclusions	Participants who had undergone prior lymphodepletion are included in the manuscript, but described in a separate cohort.
Replication	Clinical data, not applicable.
Randomization	Non-randomized
Blinding	Blinding not applicable, as not relevant in a non-randomized phase 2 study

Reporting for specific materials, systems and methods

We require information from authors about some types of materials, experimental systems and methods used in many studies. Here, indicate whether each material, system or method listed is relevant to your study. If you are not sure if a list item applies to your research, read the appropriate section before selecting a response.

Materials & experimental systems

n/a	Involved in the study
☐	☒ Antibodies
☐	☒ Eukaryotic cell lines
☒	☐ Palaeontology and archaeology
☒	☐ Animals and other organisms
☐	☒ Clinical data
☒	☐ Dual use research of concern

Methods

n/a	Involved in the study
☒	☐ ChIP-seq
☐	☒ Flow cytometry
☒	☐ MRI-based neuroimaging

Antibodies

Antibodies used

The following antibodies were used for routine phenotyping and were purchased from BD Bioscience unless otherwise noted:
PE-Cy7* anti-human PD-1 (cat. # 561272)
APC* anti-human CD45RO (cat. # 559865)
Alexa Fluor 700* anti-human CD4 (cat. # 566318)
BV421* anti-human CD27 (cat. # 562513)
BV510* anti-human CD62L (cat. # 563203)
BV650* anti-human CD8 (cat. # 563821)
BV786* anti-human CD3 (cat. # 563800)
FITC* anti-murine TCRb (cat. # 553171)
APC efluor 780* anti-murine TCRb (Ebiosciences cat. # 47-5961-82)
FITC* anti-human CD39 (Biolegend cat. # 328206)
PE* anti-human CD69 (cat. # 555531)

The following antibodies were used for TIL screening and were purchased from BD Bioscience unless otherwise noted:
FITC* anti-human CD134 (cat. # 555837)
APC* anti-human CD137 (cat. # 550890)
PE* anti-human CD4 (cat. # 347327)
APC-H7* anti-human CD3 (cat. # 641397)
Pe-Cy7* anti-human CD8 (cat. # 335787)

The following antibodies were used for TIL sorting and were purchased from BD Bioscience unless otherwise noted:
PE* anti-human CD134 (cat. # 555838)
PE* anti-human CD137 (cat. # 555956)
APC* anti-human CD4 (cat. # 340443)
FITC* anti-human CD3 (cat. # 349201)
Pe-Cy7* anti-human CD8 (cat. # 335787)

The following antibodies were used for regulatory T cell identification and were purchased from BD Bioscience unless otherwise noted:
APC* anti-human CD4 (cat. # 340443)
BV786* anti-human CD8 (cat. # 563823)
BV421* anti-human CD25 (Biolegend cat. # 302630)
BV650* anti-human GITR (cat. # 7476663)
FITC* anti-human FOXP3 (Invitrogen cat. # 11-4776-42)
PerCP Cy5.5* anti-human CD3 (Invitrogen cat. # 45-0037-42)

The following antibodies were used for ELISA assays:
anti-human IFNgamma monoclonal antibody (clone 2G1: Invitrogen cat. # M700A)
biotin labeled anti-human IFNgamma (clone B133.5: Invitrogen cat. # M701B)

Validation

Antibodies used for flow cytometry were validated using human PBMCs or human T cells transduced with TCRs expressing murine beta chain constant regions.

Eukaryotic cell lines

Policy information about cell lines and Sex and Gender in Research

Cell line source(s)

The 293GP cell line is a derivative of the 293T line and stably expresses the MoMLV (Moloney murine leukemia virus) gag/pol. The cell line was expanded into a Master Cell Bank at Indiana University Vector Production Facility in compliance with GMP regulations. Post-harvest of the supernatant, the 293GP cells are vialed and viably frozen for end-of-production cell testing or discarded.

Authentication

The 293GP cell line was tested at Indiana University Vector Production Facility to meet specifications for use in GMP manufacturing including testing for E1A antigen (293T based cell line) and ADA isoenzyme (human origin).

Mycoplasma contamination

The 293GP cell line was tested at Indiana University Vector Production Facility to meet specifications for use in GMP

Mycoplasma contamination	manufacturing including sterility, mycoplasma, adventitious viruses, human viral contaminants, identity and replication competent retrovirus. All cells were negative for mycoplasma.
Commonly misidentified lines (See ICLAC register)	None. Expression of gag-pol confirms identity of expected cell line.

Clinical data

Policy information about clinical studies

All manuscripts should comply with the ICMJE guidelines for publication of clinical research and a completed CONSORT checklist must be included with all submissions.

Clinical trial registration	NCT03412877 (clinicaltrials.gov)
Study protocol	sent to editor
Data collection	2018-2023, National Cancer Institute, Bethesda, MD
Outcomes	The primary end point of this clinical study was the objective response rate as measured using RECIST 1.1. Cross-sectional imaging was performed pretreatment, at 6 weeks post-treatment, and at regular intervals thereafter until progression. The secondary end points of the study were safety and tolerability. The exploratory end points for the study were the identification of neoantigen reactive TCRs and the feasibility of manufacturing clinical grade retroviruses and cell products. There was no pre-specified interim analysis defined in this study.

Flow Cytometry

Plots

Confirm that:

☒ The axis labels state the marker and fluorochrome used (e.g. CD4-FITC).

☒ The axis scales are clearly visible. Include numbers along axes only for bottom left plot of group (a 'group' is an analysis of identical markers).

☒ All plots are contour plots with outliers or pseudocolor plots.

☒ A numerical value for number of cells or percentage (with statistics) is provided.

Methodology

Sample preparation	PBMCs were isolated from apheresis products and small-scale blood collected in CPT tubes by density gradient separation using ficoll and were cryopreserved prior to analyses.
Instrument	Flow cytometry data were collected on a BD Canto II, a BD Fortessa, or a BD Symphony. Cells were sorted using either a BD FACs Aria or a Sony SH800S.
Software	Flow cytometry data was collected using BD FACSDiva and analyzed with FlowJo.
Cell population abundance	Data describing the pre- and post-sort cell abundance as well as the percentages of TCR transduced cells in relevant populations is presented in the text where appropriate.
Gating strategy	Lymphocytes were first gated for appropriate size by evaluating SSC-H x FSC-A. Single cells were then gated by evaluating FSC-W x FSC-H and SSC-W x SSC-H. Live (PI or DAPI negative) cells were then gated, and subsequent gating strategies are presented in the figures where appropriate.

☒ Tick this box to confirm that a figure exemplifying the gating strategy is provided in the Supplementary Information.